Desalination 555 (2023) 116562

Contents lists available at ScienceDirect

Desalination

journal homepage: www.elsevier.com/locate/desal

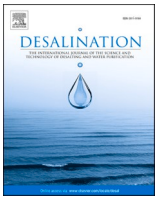

Chloride retention model for concentrated solutions containing sodium chloride and sodium sulfate based on thermodynamic considerations

Gerrald Bargeman [a,b,*], Olalla Guerra Miguez [c], Jan Barend Westerink [b], Antoon ten Kate [d]

[a] University of Twente, Faculty of Science and Technology, Membrane Science and Technology Cluster, MESA+ Institute for Nanotechnology, P.O. Box 217, 7500 AE Enschede, the Netherlands
[b] Nobian Industrial Chemicals B.V., Zutphenseweg 10, P.O. Box 10, 7400 AA Deventer, the Netherlands
[c] CZ VACCINES, CZ, Veterinaria S.A., Pol. La Relva, Torneiros s/n, 36410, O, Porriño, (Pontevedra), Spain
[d] Nouryon Chemicals B.V., Zutphenseweg 10, P.O. Box 10, 7400 AA Deventer, the Netherlands

HIGHLIGHTS

- A NaCl retention model for concentrated NaCl – Na_2SO_4 solutions was developed.
- The model is based on thermodynamic considerations.
- The membrane resistance for NaCl transport is a function of permeate NaCl activity.
- The model successfully predicted NaCl retention over a wide concentration range.
- The model can be applied for the entire range of nanofiltration membranes.

ARTICLE INFO

Keywords:
Nanofiltration
Model
Thermodynamic considerations
Chloride
Sulfate
Concentrated solutions

ABSTRACT

Modelling of nanofiltration processes focusses on dilute solutions, whereas industrial nanofiltration applications often feature the use of more concentrated solutions. Recently, nanofiltration models for dilute NaCl solutions were extended to higher concentrations of approximately 1.2 mol·L^{-1}. Furthermore, models for the prediction of the NaCl retention for saturated NaCl solutions containing impurities or anti-solvents based on thermodynamic considerations were proposed. However, proper models for intermittent NaCl concentrations were lacking. A new model, extending the earlier NaCl retention model for (near) saturated NaCl solutions, has been developed to fill the existing gap. The key assumption in the model is that the resistance for NaCl transport is a function of the sodium and chloride activities and is independent of the impurity concentration of the solution treated. Based on the experimental results generated in this study and obtained from open literature the validity of this model has been proven for NaCl solutions containing Na_2SO_4. Experimental NaCl retentions could be predicted by the developed model with sufficient accuracy (within 5 % absolute) over a wide range of NaCl and Na_2SO_4 concentrations up to saturation. The largest inaccuracies were obtained for nanofiltration of (near) saturated NaCl solutions at very low membrane flux.

1. Introduction

Nanofiltration (NF) is a pressure-driven membrane technology applying membranes often consisting of a thin film composite layer produced via interfacial polymerization or polyelectrolyte multilayer deposition on an ultrafiltration membrane support [1–3]. These NF membranes are characterized by a molecular weight cut-off between 200 and 1000 Da, thus showing a molecular weight cut-off in between those for reverse osmosis and ultrafiltration membranes [1]. The retention of nanofiltration membranes for ionic and neutral solutes is generally considered to be a result of a combination of separation mechanisms such as size exclusion, Donnan exclusion and di-electric exclusion [4–9]. Several transport models describing solvent flux and solute retention have been developed and reported since the introduction of nanofiltration membranes in the mid-nineties of the previous century [1]. Usually, an extended Nernst-Planck based Donnan Steric

* Corresponding author at: University of Twente, Meander building, PO Box 217, 7500 AE, Enschede, the Netherlands.
E-mail address: g.bargeman@utwente.nl (G. Bargeman).

https://doi.org/10.1016/j.desal.2023.116562
Received 19 January 2023; Received in revised form 6 March 2023; Accepted 9 March 2023
Available online 20 March 2023

Pore – Di-electric Exclusion (DSPM-DE) model or a Maxwell-Stefan based model are used to describe the transport of the solvent and solutes through the membrane [4–8]. These models are often applied for nanofiltration of dilute solutions (usually with concentrations below 0.1 mol·L^{-1}), where Donnan exclusion and di-electric exclusion play an important role for the selective transport of the ionic solutes [4–6,10]. The focus on nanofiltration of dilute solutions in scientific literature stems from the intention of scientists to characterize nanofiltration membranes in terms of their pore radius (distribution), effective thickness, charge density, and di-electric constant. This type of information is amongst others used to unravel the effect of interactions between individual solutes and interactions between the membrane and individual solutes on membrane flux and solute retention. Based on these insights nanofiltration membrane performance at other conditions than experimentally evaluated is predicted using the models mentioned earlier [11–17]. Several studies have shown that a lot of phenomena close to and inside the membrane happen simultaneously, and a proper fundamental description of these types of phenomena such as the effect of salt concentration on retention of other solutes is not straightforward [11–15,17].

In recent years efforts have been devoted to generating methods and models to describe the transport through nanofiltration membranes for solutions closer to those applied in industry, often featuring higher concentrations of solutes such as salt ions [11,18–23] and/or sugars [24–26]. Next to the separation of neutral compounds such as sugars [24–26], or the separation of neutral and charged compounds (such as glucose and salt, often NaCl) [11,14,27], nanofiltration for the separation of chlorides and sulfates from concentrated solutions has received growing attention as well [19,20,28–30]. This separation is important for applications such as nanofiltration of sea water (for the generation of sulfate lean injection water for enhanced oil and gas production), of retentates from water production using reverse osmosis of sea water (for example in zero-liquid discharge processes), of depleted brines from chlor-alkali production (for minimizing the discharge of sulfate containing purge streams) and of brines obtained during salt production [18,19].

Perez-Gonzalez et al. [20] performed nanofiltration experiments using NaCl – Na_2SO_4 mixed solutions with NaCl concentrations between 0.2 and 1.2 mol·L^{-1}. Ortiz-Albo et al. used [30] these experimental results to successfully validate their developed extended method using zeta potential results to calculate surface charge densities and subsequently predicting the sulfate and chloride retention applying the well-known Donnan Steric Pore Model (DSPE). Consequently, predictive models for the separation of sodium sulfate from sodium chloride using nanofiltration membranes have become available for the NaCl concentration range in between 0 and 1.2 mol·L^{-1}. Bargeman et al. [19,28] and ten Kate et al. [29] described the transport of chloride through nanofiltration membranes processing (near) saturated NaCl solutions (with a NaCl concentration higher than 5 mol·L^{-1}) containing other co-ions, including Na_2SO_4, or neutral compounds that act as co-solvent or anti-solvent. These authors modelled the NaCl retention based on an experimentally derived empirical correlation [19] or based on thermodynamic considerations assuming that the resistance for NaCl transport through the membrane and the effect of the pressure difference between concentrate and permeate is negligible, and that either the NaCl activity coefficients on both sides of the membrane are the same [28] or that these coefficients can be obtained from solid-liquid equilibria (crystallization experiments) [29]. Their approach was proven suitable for nanofiltration of solutions (practically) saturated in NaCl, producing concentrates and permeates (practically) saturated in NaCl and in some cases even supersaturated in Na_2SO_4 [19,28,29].

However, based on the above it is evident that for mixed NaCl – Na_2SO_4 solutions the models available for the prediction of the NaCl retention shows a gap in the NaCl concentration range between 1.2 and 5 mol·L^{-1}. This concentration range is important for several nanofiltration applications. These applications include processing of RO retentates from seawater desalination and depleted brines from chlor-alkali production [18] and purifying salty waste streams in zero-liquid discharge concepts to produce NaCl streams with low impurity concentrations which can be concentrated via osmotically assisted reverse osmosis or alternative concentration technologies [31]. It is therefore important to develop methods to predict the NaCl retention for solutions in this concentration range, which is the goal of the work described in this manuscript. This newly developed model will be based on and will extend the earlier proposed thermodynamically based models for nanofiltration of (near) saturated salt solutions [28,29].

In the next sections theoretical considerations, the developed model, and experiments to validate the developed model will be described. In subsequent sections model and experimental results will be reported, compared, and discussed, and conclusions will be drawn.

2. Theoretical considerations and model development

2.1. Available retention model for saturated NaCl salt solutions

One of the key parameters for the feasibility of nanofiltration processes is the retention of the nanofiltration membrane. This retention is defined according to:

$$R_i = \left(1 - \frac{c_{i,p}}{c_{i,c}}\right) \tag{1}$$

For saturated NaCl solutions the transport of sodium chloride through nanofiltration membranes has been described based on thermodynamical considerations [28]. The resistance for the transport through the membrane, leading to a chemical potential difference between the concentrate side and the permeate side of the membrane of $\Delta\mu_{membr,i}$, was described according to [28,29]:

$$\mu_i(x,P,T)_c = \mu_i(x,P,T)_p + \Delta\mu_{membr,i} \tag{2}$$

The effect of pressure and temperature on the chemical potential can be shown explicitly via Eq. (3) and Eq. (4) [28,29].

$$\mu_i(x,P_0,T)_c + V_{m,c,i}\cdot(P_c - P_0) = \mu_i(x,P_0,T)_p + V_{m,p,i}\cdot(P_p - P_0) + \Delta\mu_{membr,i} \tag{3}$$

$$\mu^*_{NaCl} + R\cdot T\cdot(lna_{Na^+} + lna_{Cl^-})_c = \mu^*_{NaCl} + R\cdot T\cdot(lna_{Na^+} + lna_{Cl^-})_p - V_{m,p,NaCl}\cdot(P_c - P_p) + \Delta\mu_{membr,NaCl} \tag{4}$$

In Eq. (4) the Eq. (3) has been specified for i = NaCl and it has been assumed that the molar volumes for NaCl at the concentrate and permeate side of the membrane are equal. Furthermore, rearranging Eq. (4) leads to the following relation between the Na^+ and Cl^- activity ratio in concentrate over permeate of:

$$\frac{(a_{Na^+}\cdot a_{Cl^-})_c}{(a_{Na^+}\cdot a_{Cl^-})_p} = e^{\frac{\Delta\mu_{membr,NaCl} - V_{m,p,NaCl}\cdot(P_c - P_p)}{R\cdot T}} \tag{5}$$

Since activity coefficients for ionic solutions are usually based on molality, for example those obtained from the Pitzer model [32,33], Eq. (5) can be expressed according to:

$$\frac{(\gamma_{Na^+}\cdot\gamma_{Cl^-})_c}{(\gamma_{Na^+}\cdot\gamma_{Cl^-})_p}\frac{(m_{Na^+}\cdot m_{Cl^-})_c}{(m_{Na^+}\cdot m_{Cl^-})_p} = e^{\frac{\Delta\mu_{membr,NaCl} - V_{m,p,NaCl}\cdot(P_c - P_p)}{R\cdot T}} \tag{6}$$

Replacing the individual ion-activity coefficients by the mean salt activity coefficient leads to:

$$\frac{\gamma^2_{NaCl,c}}{\gamma^2_{NaCl,p}}\frac{(m_{Na^+}\cdot m_{Cl^-})_c}{(m_{Na^+}\cdot m_{Cl^-})_p} = e^{\frac{\Delta\mu_{membr,NaCl} - V_{m,p,NaCl}\cdot(P_c - P_p)}{R\cdot T}} \tag{7}$$

For saturated NaCl solutions containing Na_2SO_4 in the earlier study [28], the effect of the difference in pressure between the concentrate and permeate side was neglected and the resistance of the membrane for NaCl transport was assumed to be negligible as well, leading to the assumption that $\Delta\mu_{membr,NaCl} \approx 0$. Furthermore, the authors [28] assumed

that the ratio of the activity coefficients for Na^+ and Cl^- in the concentrate and the permeate, and the ratio of the total molecule concentration in the concentrate and permeate were equal to 1 for these (practically) saturated solutions. This led to a further simplification of Eq. (5) and Eq. (7) to:

$$\frac{(c_{Na^+}\cdot c_{Cl^-})_c}{(c_{Na^+}\cdot c_{Cl^-})_p} \approx 1 \tag{8}$$

It was shown that this model was able to predict the NaCl retention for nanofiltration of saturated NaCl solutions containing Na_2SO_4 reasonably well [28]. Alternatively, in [29] which describes a retention model using a similar approach but extending it to other impurities in the NaCl solution, it was shown that the activity coefficients could be obtained from solid-liquid equilibrium results (NaCl crystallization experiments).

2.2. Aim of the extended NaCl retention model and assumptions made

The aim of the current work is to extend the model described above to nanofiltration of concentrated NaCl solutions containing Na_2SO_4 with a NaCl concentration between 1.5 mol·L^{-1} and saturation (approximately 5.5 mol·L^{-1}, depending on the sulfate concentration). This NaCl concentration range reflects nanofiltration of solutions produced as retentates from reverse osmosis of sea water, depleted brines from chlor-alkali production and brines obtained during salt production [18,19], as mentioned earlier. Consequently, the assumptions related to the negligible membrane resistance, the negligible pressure-difference between concentrate and permeate, the activity coefficient ratio being equal to 1 and the equal total compound concentration in the concentrate and permeate as made in the available model [28] do not necessarily hold.

In the extended model, described in the current work, these assumptions are therefore not made and the starting point for the prediction of the NaCl retention will be Eq. (7). The use of this equation means that values for NaCl activity coefficients, molar volumes for NaCl, Na_2SO_4 and water for the permeate, the Na_2SO_4 retention, the molality for Na^+, Cl^- and SO_4^{2-} in the concentrate and $\Delta\mu_{membr,NaCl}$ need to be available or determined to obtain the molality for Na^+, Cl^- and SO_4^{2-} for the permeate. Based on the obtained molality for Na^+ and Cl^- in the permeate, the mole fractions and concentrations of these ions can be calculated, and the chloride retention (also referred to as NaCl retention in the remainder of this manuscript) can be obtained. The methodology used to generate activity coefficient and molar volume data will be presented in the next sections.

In the currently described extended model, it has been assumed that $\Delta\mu_{membr,NaCl}$, reflecting the resistance for NaCl transport through the membrane, is a function of the NaCl activity in the permeate according to:

$$\Delta\mu_{membr,NaCl} = f\left(\sqrt{(a_{Na^+}\cdot a_{Cl^-})_p}\right) \tag{9}$$

The basis for this assumption is that in Maxwell-Stefan modelling approaches it is assumed that the resistance for transport occurs due to velocity differences inside the membrane (creating friction between the individual solutes, the solvent and the individual solutes, and between the individual solutes and the solvent with the membrane) and the distribution of components at the boundary of the membrane and the liquid is described by an equilibrium (Donnan equilibrium, di-electric exclusion and size exclusion) [4]. Ideally, the friction inside the membrane is described as a function of local concentrations for very dilute solutions, or as a function of local activities for more concentrated solutions such as studied here. However, especially for more concentrated solutions, this approach would require activity coefficient data inside the membrane, which is not easily obtained or derived. Consequently, in this work the approach has been to base the resistance for NaCl transport on the activity of sodium and chloride in the permeate, since it was expected that this would reflect the situation best. To validate whether this assumption has a strong effect on the predicted NaCl retention, the Supporting Information provides information on results that have been obtained assuming that $\Delta\mu_{membr,NaCl}$ is a function of the NaCl activity in the concentrate instead of the permeate. These results in the Supporting Information (see section SI.3) clearly show that the predicted $\Delta\mu_{membr,NaCl}$ and NaCl retention for NaCl – Na_2SO_4 mixture solutions over the entire concentration range evaluated are independent on whether $\Delta\mu_{membr,NaCl}$ is expressed as a function of the sodium and chloride activities in permeate or in the concentrate.

If $\Delta\mu_{membr,NaCl}$ is assumed to be a function of the NaCl activity of the permeate only, it can be obtained based on NaCl retention results from experiments using single NaCl solutions if activity coefficient data, NaCl and H_2O molar volume data and solution densities as function of the NaCl concentration are available.

2.3. Activity coefficients

The activity coefficients required in the model have been obtained from the correlations proposed by Pitzer and co-workers [32,33], and the values for the required single salt and interaction parameters A^{φ}, b, $\beta^{(0)}$, $\beta^{(1)}$, C^{φ}, ϑ_{ClSO_4} and ψ_{NaClSO_4} as provided therein. The equations proposed by these authors extended the original Debye-Hückel method [32,33]. For several decades, the correlations proposed by Pitzer have been successfully used in membrane science studies (see e.g. [34–38]) to predict osmotic coefficients and activity coefficients for many mixed electrolyte solutions.

Activity coefficients obtained from the calculation procedure based on the Pitzer correlations have been successfully validated against experimentally determined activity coefficient results as reported by Sirbu et al. [39] (see Supporting Information Fig. S1). These authors presented experimentally determined activity coefficients for a range of mixed NaCl – Na_2SO_4 solutions with ionic strengths between I = 0.1–4 mol·kg water^{-1} and a Na_2SO_4 induced ionic strength over total ionic strength ratio range of $y_{Na_2SO_4}$ = 0–0.8 [39]. Consequently, since we have only extended the concentration range of the NaCl – Na_2SO_4 solutions to a limited extent, we have assumed that the activity coefficients obtained from the Pitzer correlations can be applied for the estimation of the activities of the NaCl – Na_2SO_4 solutions concentration range evaluated our modelling activity as well. It should be noted that in the currently proposed model instead of the Pitzer correlations newly developed electrolyte models for the determination of the NaCl activity coefficients (see e.g. [40,41]) can be applied as well if users of our proposed model description so desire. In our work, the Pitzer model approach was selected merely because of its proven accuracy for NaCl – Na_2SO_4 solutions [39] and because it is well known and widely applied in membranes science, as discussed earlier in this section.

2.4. Molar volume and solution density

The molar volume of the solutions has been determined using Masson's rule according to:

$$V_{m,sol} = \sum_i x_i \cdot V_{m,i} \tag{10}$$

$$V_{m,i} = V_{m,i,0} + V_{m,i,1}\cdot c_i^{0.5} \quad \text{for } i = \text{NaCl} \quad \text{or } Na_2SO_4 \tag{11}$$

$$V_{m,H_2O} = 0.01805\ L\cdot mol^{-1} \tag{12}$$

The solution density can be determined from:

$$\rho_{sol} = \frac{\sum_i x_i \cdot M_{w,i}}{V_{m,sol}} \tag{13}$$

Substituting Eq. (10) into Eq. (13) leads to the following equation for the solution density:

$$\rho_{sol} = \frac{\sum_i x_i \cdot M_{w,i}}{\sum_i x_i \cdot V_{m,i}} \tag{14}$$

Furthermore, the concentration and the mole fraction of component i are related according to:

$$x_i = c_i \cdot V_{m,sol} \tag{15}$$

since the sum of all molar fractions equals unity, the following applies:

$$V_{m,sol} \cdot \sum_i c_i = 1 \tag{16}$$

Substituting Eq. (15) into Eq. (14) results in:

$$\rho_{sol} = \frac{\sum_i c_i \cdot M_{w,i}}{\sum_i c_i \cdot V_{m,i}} \tag{17}$$

Furthermore, substituting Eq. (15) into Eq. (10) and rearranging this obtained relation leads to:

$$\sum_i c_i \cdot V_{m,i} = 1 \tag{18}$$

Introducing this equation into Eq. (17) lead to the following equation for the solution density:

$$\rho_{sol} = \sum_i c_i \cdot M_{w,i} \tag{19}$$

This means that when the salt concentrations in the solution are known, the component molar volumes can be determined from Eq. (11) and Eq. (12) and subsequently, the water concentration can be determined from Eq. (18), the molar volume of the solution can be determined from Eq. (16) and the solvent density can be determined from Eq. (19).

Parameters for the different compounds as required in Eq. (11) used to determine molar volumes for NaCl and Na_2SO_4, are listed in Table 1. These parameters have been obtained in this study by experimentally determining densities for single salt NaCl and Na_2SO_4 solutions and salt NaCl – Na_2SO_4 mixture solutions with defined concentrations, applying Eq. (11), Eq. (12), Eq. (18), Eq. (19) and a partial least square fitting method.

2.5. Determination of $\Delta\mu_{membr,NaCl}$ as function of the NaCl activity based on single salt NaCl solution experiments

The chemical potential difference between the concentrate and permeate $\Delta\mu_{membr,NaCl}$ has been determined for specific conditions and NaCl concentrations, according to the model represented in Fig. 1. It has been assumed that the NaCl concentration of the concentrate, an input variable, is known, and the concentration of the permeate is determined from a relation between the NaCl retention and the concentrate NaCl concentration. This relation has been determined from experimental results (see Eq. (32) in the results section). The NaCl molar volumes of the concentrate and permeate have been determined using Masson's rule based on the NaCl concentration for the concentrate and the permeate via Eq. (11) presented in the previous section. Subsequently, using the molar volume of water (see Eq. 12), and the water concentration of the permeate and concentrate, which have been calculated using Eq. (18), the NaCl molality for the permeate and concentrate have been calculated according to:

Table 1
Parameters required in Eq. (11) for NaCl and Na_2SO_4.

Compound	$V_{m,i,0}$	$V_{m,i,1}$
	$L \cdot mol^{-1}$	$L \cdot mol^{-1.5}$
NaCl	0.01593	0.002253
Na_2SO_4	0.009733	0.01309

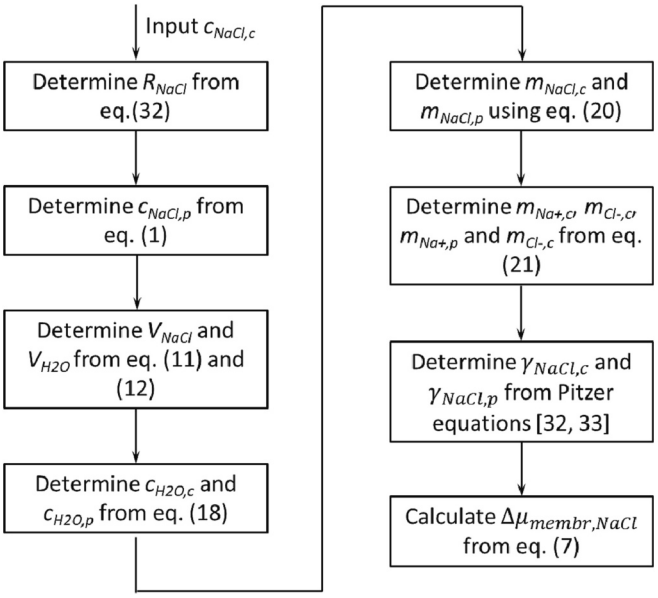

Fig. 1. Schematic representation of the calculation procedure to determine the chemical potential difference between the concentrate and permeate side of the nanofiltration membrane for a single salt NaCl solution.

$$m_{i,j} = \frac{c_{i,j} \cdot 1000}{c_{H_2O,j} \cdot M_{H_2O}} \quad \text{for } i = \text{NaCl and } j = c \text{ or } p \tag{20}$$

The conversion factor of 1000 used in Eq. (20) is a result of expressing the molecular weight of water in $g \cdot mol^{-1}$ and the commonly used unit for molality of $mol \cdot kg^{-1}$.

The molality for the individual ions (Na^+ and Cl^-) for the single salt NaCl solution has been determined according to:

$$m_{Cl^-} = m_{Na^+} = m_{NaCl} \tag{21}$$

After substituting the activity coefficients, which have been calculated based on the Pitzer equations as described in a previous section, the Na^+ and Cl^- molality values for the permeate and concentrate, the NaCl molar volume for the permeate, the concentrate and permeate pressures, and the temperature in Eq. (7), $\Delta\mu_{membr,NaCl}$ has been obtained.

After determination of $\Delta\mu_{membr,NaCl}$ for a variety of NaCl concentrations in the feed solution, this chemical potential difference has been correlated to the NaCl activity in the permeate for single NaCl salt solutions according to Eq. (9). As mentioned earlier, it was assumed in the extended model that this relation will also apply to the nanofiltration process processing a concentrated NaCl – Na_2SO_4 mixture saturated or undersaturated in NaCl for the concentration range specified earlier.

2.6. Determination of the NaCl retention for concentrated NaCl – Na_2SO_4 mixtures based on $\Delta\mu_{membr,NaCl}$ determined from single NaCl salt retentions

The NaCl retention for a concentrated NaCl – Na_2SO_4 mixture saturated or undersaturated in NaCl can be predicted from the NaCl and Na_2SO_4 concentrations in the concentrate and the Na_2SO_4 retention as schematically shown in Fig. 2 and explained below. The extended NaCl retention model contains several procedures. The first two (parallel) procedures are related to the calculation of the concentrate and permeate NaCl and Na_2SO_4 molality, and NaCl activity coefficients. These procedures resemble the molality calculation procedure discussed in the previous section for the single NaCl salt solution, apart from the introduction of the second salt, (Na_2SO_4) and the fact that the NaCl retention and the NaCl concentration in the permeate are output parameters instead of input parameters.

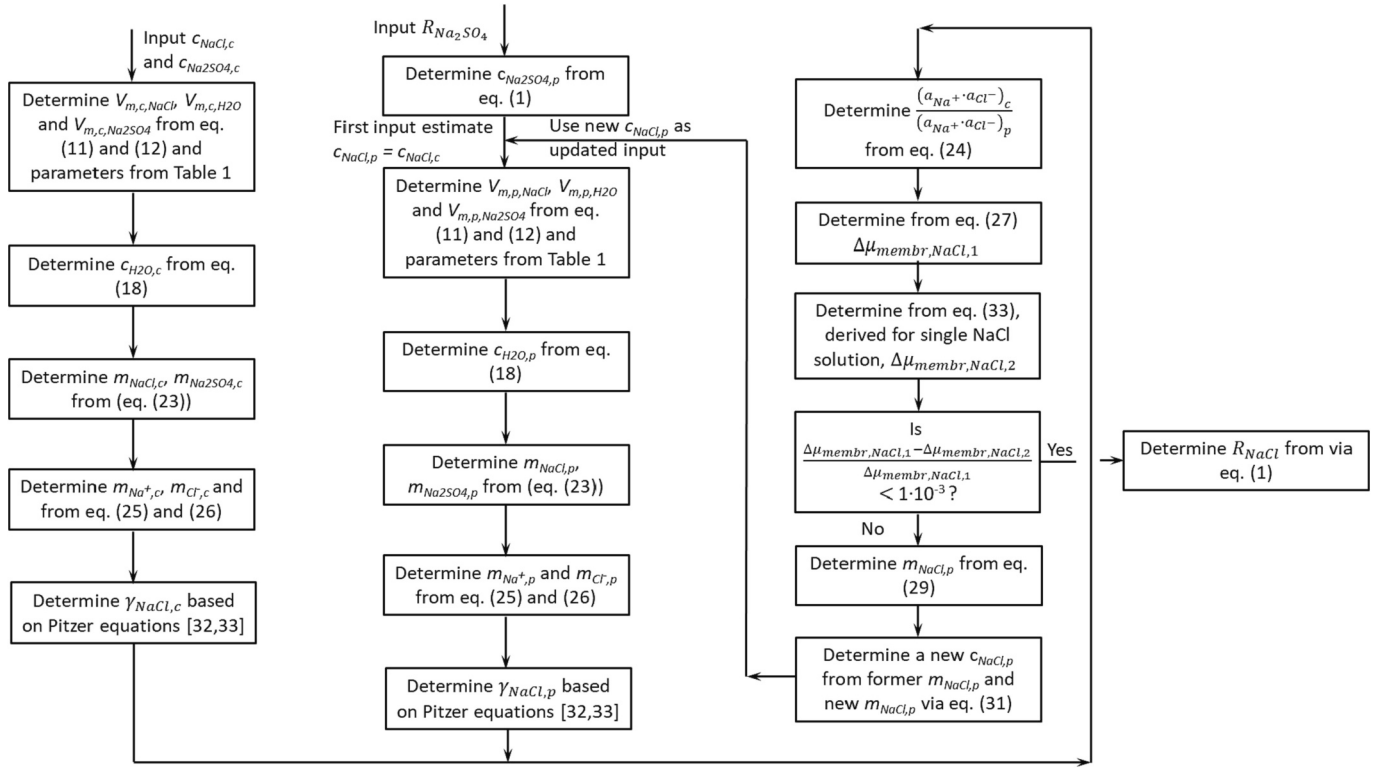

Fig. 2. Schematic representation of the procedure used to determine the NaCl retention for nanofiltration of a mixed salt NaCl – Na_2SO_4 solution containing >0.9 mol·L^{-1} NaCl based on the chemical potential drop for NaCl transport as function of the permeate NaCl activity obtained from single NaCl solution retentions.

The Na_2SO_4 concentration in permeate can be obtained from the measured or assumed Na_2SO_4 retention via Eq. (1). Since the NaCl retention is the desired output variable from the modelling and the NaCl concentration in the permeate is an output parameter as well, a first estimate for the NaCl concentration in the permeate needs to be provided to an iteration loop for the calculation of the permeate molalities and NaCl activity coefficients. As a first estimate it is assumed that the NaCl concentration in the permeate is equal to that in the concentrate:

$$c_{NaCl,p} = c_{NaCl,c} \tag{22}$$

The NaCl and Na_2SO_4 molalities for the permeate and the concentrate can be calculated according to:

$$m_{i,j} = \frac{c_{i,j}\cdot 1000}{c_{H_2O,j}\cdot M_{H_2O}} \quad \text{for } i = \text{NaCl or } Na_2SO_4 \text{ and } j = c \text{ or } p \tag{23}$$

The required water concentration for the permeate and concentrate can be determined from Eq. (11), Eq. (12) and Eq. (18) applying Masson's rule.

Subsequently, the NaCl activity coefficients can be obtained from the correlations presented by Pitzer and Kim [33].

The ratio of the activity for NaCl in the concentrate over the permeate can be determined from:

$$\frac{(a_{Na^+}\cdot a_{Cl^-})_c}{(a_{Na^+}\cdot a_{Cl^-})_p} = \frac{\gamma^2_{NaCl,c}}{\gamma^2_{NaCl,p}}\cdot\frac{(m_{Na^+}\cdot m_{Cl^-})_c}{(m_{Na^+}\cdot m_{Cl^-})_p} \tag{24}$$

where:

$$m_{Na^+} = m_{NaCl} + 2\cdot m_{Na_2SO_4} \tag{25}$$

and

$$m_{Cl^-} = m_{NaCl} \tag{26}$$

The chemical potential difference for NaCl transport can be obtained by rearranging Eq. (5). This leads to:

$$\Delta\mu_{membr,NaCl} = V_{m,p,NaCl}\cdot\left(P_c - P_p\right) + \mathrm{R}\cdot\mathrm{T}\cdot ln\frac{(a_{Na^+}\cdot a_{Cl^-})_c}{(a_{Na^+}\cdot a_{Cl^-})_p} \tag{27}$$

Furthermore, it has been assumed earlier that the $\Delta\mu_{membr,NaCl}$ is only dependent on the NaCl activity in permeate and has been determined from single salt NaCl solution experiments. For the break-up criterion of the NaCl permeate concentration calculation loop (see Fig. 2) the allowable relative deviation in the chemical potential difference is assumed to be $\frac{\Delta\Delta\mu_{membr,NaCl}}{\Delta\mu_{membr,NaCl}} < 10^{-3}$. In this criterion $\Delta\Delta\mu_{membr,NaCl}$ is the difference between $\Delta\mu_{membr,NaCl}$ calculated via Eq. (27) and $\Delta\mu_{membr,NaCl}$ calculated based on the correlation determined from the single NaCl salt experiments (Eq. (33)). If this criterion is not met, the NaCl permeate concentration needs to be adapted according to the procedure described below.

Based on Eqs. (25) and (26) the Na^+ and Cl^- molality product can be determined according to:

$$\left(m_{Na^+,p}\cdot m_{Cl^-,p}\right) = \left(m_{NaCl,p} + 2\cdot m_{Na_2SO_4,p}\right)\cdot m_{NaCl,p} \tag{28}$$

Rearranging this equation and specifying it for the permeate solution leads to:

$$m_{NaCl,p} = -m_{Na_2SO_4,p} + \sqrt{\left(m^2_{Na_2SO_4,p} + (m_{Na^+}\cdot m_{Cl^-})_p\right)} \tag{29}$$

The Na^+ and Cl^- molality product can be obtained from:

$$(m_{Na^+}\cdot m_{Cl^-})_p = \frac{\gamma^2_{NaCl,c}}{\gamma^2_{NaCl,p}}\cdot\frac{(m_{Na^+}\cdot m_{Cl^-})_c}{e^{\frac{\Delta\mu_{membr,NaCl}-V_{m,NaCl}\cdot(P_c-P_p)}{R\cdot T}}} \tag{30}$$

where $\Delta\mu_{membr,NaCl}$ is based on the correlation between the chemical potential difference for NaCl transport as obtained from single NaCl salt solution experiments (Eq. (33)) and the earlier determined NaCl molality and activity coefficient. Furthermore, the Na_2SO_4 molality in permeate ($m_{Na_2SO_4,p}$) can be obtained from the sulfate retention.

With the updated (new) value for the NaCl molality of the permeate

as determined from Eq. (29) an updated (new) NaCl concentration for the permeate can be determined according to:

$$c_{NaCl,p,k+1} = \frac{\left(0.6 \cdot m_{NaCl,p,k} + 0.4 \cdot m_{NaCl,p,k+1}\right)}{m_{NaCl,p,k}} \cdot c_{NaCl,p,k} \quad (31)$$

This updated concentration is fed as input to the calculation procedure, which is repeated until the earlier mentioned break-up criterion $\frac{\Delta\Delta\mu_{membr,NaCl}}{\Delta\mu_{membr,NaCl}} < 10^{-3}$ is met (see Fig. 2) and the NaCl concentration in the permeate and consequently the NaCl retention is available.

3. Experimental

3.1. Equipment

Experiments were performed using a DSS Labstak M20 unit as described by van der Horst et al. [42] and Bargeman et al. [11,28]. In the DSS Labstak M20 unit type used, the liquid feed was supplied to the top of the membrane stack, flowing downwards to the outlet at the bottom of the stack. During the experiments both the retentate and the permeate were recycled to the feed vessel. This mode of experimentation is called full-recycle operation. Several (up to ten) membranes were placed in series, each membrane having a surface area of 0.036 m^2.

3.2. Membrane specifications

Nanofiltration membranes from different suppliers as listed in Table 1 and further specified below were evaluated. Desal 5DK and Desal 5HL (GE Water Technologies) are three-layer thin film polysulfone based membranes with a polyamide top layer [12]. NP030 (NADIR) is a permanently hydrophilic polyethersulfone membrane, suitable for extreme pH conditions (pH = 0–14). This material is claimed to provide a broad chemical compatibility [43]. MPF 34 (Koch) is a flat sheet proprietary composite nanofiltration membrane, representative for spiral wound module MPS 34 [44]. The membrane is suitable for operation at extreme pH conditions (between 0 and 14). UTC 60 (Toray Industries, ROMEMBRA) is a cross-linked polyamide composite membrane which is positively charged [45]. NTR-7410, NTR-7450 and NTR-7470 (SOMICON, Nitto Denko) are negatively charged sulfonated polyethersulfone composite membranes [46], whereas NTR-7250 (SOMICON, Nitto Denko) is a negatively charged polyvinyl alcohol/polyamide composite membrane. NF 270 (Dow) is a polyamide thin-film composite, which is negatively charged [10]. The molecular weight cut-offs (MWCO), $MgSO_4$, NaCl and Na_2SO_4 retentions and the permeabilities of these membranes as reported by the suppliers or quoted in other studies as supplier information are listed in Table 2.

3.3. Membrane experiments

Prior to the experiments using salt solutions as feedstock, the membranes were pre-compacted by increasing the pressure to $P = 25$ bar and maintaining full-recycle operation at this pressure for 1 h. During the pre-compaction at a temperature of 20 °C, and a crossflow rate of 515 $L{\cdot}h^{-1}$ de-mineralized water was used as feed.

All subsequent experiments were performed at $T = 21\ °C \pm 2\ °C$, using trans-membrane pressures of 5, 10, 20 or 25 bar, and a crossflow between 600 and 800 $L{\cdot}h^{-1}$. Since the combined permeate flows of the membranes was always <7 % of the retentate flow, the crossflow rate was practically equal for all the membranes and concentration changes along the retentate side of the membrane stack, even for compounds with high retention, were limited. The pressure-drop along the feed/concentrate side of the module was 1 bar during all experimental conditions. This pressure drop was accounted for in the calculation of trans-membrane pressures for the individual membranes. After each pressure adjustment stabilization of membrane performance was allowed for at least 60 min before flux and retention measurements were performed. At each experimental condition the permeate flux, and retentate and permeate compositions were determined.

Prior to nanofiltration using salt solutions, pure water fluxes were measured using de-mineralized water to determine the permeances of the individual membranes and to validate these against available supplier or open literature information. Salt solutions for the nanofiltration experiments were prepared by dissolving NaCl, Na_2SO_4 or a combination of the two salts in de-mineralized water. NaCl was obtained from Sigma Aldrich (The Netherlands), while Na_2SO_4 was obtained from Mallinckrodt Baker B.V. (The Netherlands). Experiments using single salt solutions prepared by dissolving NaCl in de-mineralized water were performed at concentrations between 0.058 $g{\cdot}L^{-1}$ and 300 $g{\cdot}L^{-1}$. To

Table 2
Membrane characteristics as reported by membrane suppliers or quoted by other studies as supplier information.

Membrane	Ratio flux/pressure ($L{\cdot}m^{-2}{\cdot}h^{-1}{\cdot}bar^{-1}$)	NaCl retention (%)	Na_2SO_4 retention (%)	$MgSO_4$ retention (%)	MWCO (Da)	Retention neutral solute (%)
Desal 5DK	5.5[a]			98[a]	200 [12]	
Desal 5HL	6.7[a]			98[a]	150–300	
NP 030	> 1	25-35[d]	80-95[d]		400[e]	
MPF 34	2	35[f]			200–300	95 (glucose)/97 (sucrose)[g]
UTC 60	2.2 [47]	63.6[i] [48]	99.6[h] [48]			92 (glucose) [47]
						94 (sucrose) [47]
						92 (raffinose) [47]
						95.4[h] (glucose) [48]
NTR-7410	50 [10,46]	15 [46]				15 (sucrose) [10,46]
NTR-7450	10 [10]	51 [10]				36 (sucrose) [10]
NTR-7470		70[j] [49]			200–250 [49]	
NTR-7250	4[b]	50				
	16.4 [10,46]	60 [10,46]				94 (glucose) [46]
NF270	11[c]			97[c]		

[a] Using a 2000 $mg{\cdot}L^{-1}$ $MgSO_4$ solution at 6.9 bar, 25 °C and 15 % recovery.
[b] Using a NaCl solution at standard conditions (not specified).
[c] Using a 2000 $mg{\cdot}L^{-1}$ $MgSO_4$ solution at 4.8 bar, 25 °C and 15 % recovery.
[d] Test conditions: 40 bar, 20 °C, stirred cell (700 rpm). Retention of Na_2SO_4 for processing of a 0.5 % Na_2SO_4 solution. Retention of NaCl processing a 0.5 % NaCl solution.
[e] Based on the reported lactose retention from stirred cell experiments.
[f] Using a 5%NaCl solution at 30 bar and 30 °C.
[g] Using a 3 % glucose / 3 % sucrose solution at 30 bar and 30 °C.
[h] Using a 0.15 % solution at 15 bar pressure.
[i] Using a 0.05 % solution at 15 bar pressure.
[j] Using a 0.15 % solution at a temperature of 25 °C.

investigate the influence of the presence of Na_2SO_4 on NaCl retention and vice versa, experiments were carried out using mixtures of NaCl (with a concentration in the range of 90–295 g·L^{-1}) and Na_2SO_4 (with a concentration in the range of 5–150 g·L^{-1}). At the end of the experimental program using NaCl/Na_2SO_4 solutions, nanofiltration experiments with a 0.058 g·L^{-1} NaCl solution and with demineralized water were repeated to evaluate whether the membrane characteristics had changed, or membranes had compacted.

Chloride concentrations were analyzed by titration using a Metrohm titration-processor adding $AgNO_3$ to the sample [11,28]. The sulfate concentrations were analyzed using inductively coupled plasma emission spectroscopy (ICP-ES) or alternatively using ion chromatography (DX120 – AS9HC column system – 9 mM CO_3^{2-} - 25 μL loop). For single salt solutions the chloride retentions were based on conductivity measurements using a WTW conductivity measurement system, producing values applicable at a room temperature of 20 °C, as well. The density of samples was measured by weighing a known sample volume.

4. Results and discussion

4.1. Experimental results single NaCl salt solutions

Membrane retentions for several commercially available NF membranes for single salt solutions with NaCl concentrations between 99 g·L^{-1} and 290 g·L^{-1} NaCl are below 17 % (see Fig. 3 and Fig. S2 in the Supporting Information). The retentions for Desal DK, Desal HL and NF-270 are generally reducing with increasing NaCl concentration in this concentration range and seem to be hardly dependent on the membrane type used (see Fig. 3). The NaCl retention is a function of the membrane flux at relatively low flux and stabilizes at higher flux if concentration polarization does not play a major role. This is in line with the usually observed NaCl retention – flux behavior for solutions with lower NaCl concentrations [4,50].

Based on the NaCl retention results as function of the NaCl concentration in the concentrate as published by Bargeman et al. [11] and Tanninen et al. [50] for different nanofiltration membranes and experimental results obtained in the current experimental program, it is evident that at a flux of 25 L·m^{-2}·h^{-1} the NaCl retention is relatively low (below 15 %) for NaCl concentrations in concentrate of 0.9 mol·L^{-1} and higher (see Fig. 4). The NaCl retention for single NaCl solutions (R_{NaCl} in % and $c_{NaCl,c}$ in mol·L^{-1}) for Desal DK at a flux of approximately 25 L·m^{-2}·h^{-1} can be approximated by the trend line presented in Fig. 4 (left), yielding:

$$R_{NaCl} = 13.5 - 6.04 \cdot ln\left(c_{NaCl,c}\right) \quad (32)$$

Although the NaCl retention for different nanofiltration membranes (Desal HL, NF-270 and NTR-7250) at constant NaCl concentration is slightly different, as a first estimate it is assumed that this relation for Desal DK also applies for these other nanofiltration membranes, despite the small deviation of the NaCl retentions from this relation (see Fig. 4 (right)).

Results for other membranes evaluated can be found in the Supplementary Information. The NaCl retentions for these membranes (NTR-7450, NTR-7470, NP-030, UTC 60) are equal to slightly lower than those for NTR-720 (see Figs. S2 and S3 in the Supporting Information) at the same NaCl concentration in the concentrate and the same flux. Consequently, Eq. (32) describes the single NaCl retention at a flux of 25 L•m^{-2}•h^{-1} for tight nanofiltration membranes [11,28] such as Desal DK, Desal HL, NF-270 and NTR-7250. Furthermore, for relatively open nanofiltration membranes such as NTR-7470, NTR-7450, NP-030 and UTC 60, this equation provides a proper, but slightly higher than observed, first estimate for the NaCl retention for single NaCl solutions at the earlier mentioned flux. The small difference in the NaCl retention between the tightest nanofiltration membranes (NF-270, Desal DK, NTR-7250 and Desal HL) is due to a combination of effects. These membranes have similar pore radii and the ratio of the solute radius over pore radius for these membranes increases (up to 20 %) similarly for these membranes with increasing NaCl concentration, as found during membrane characterization [11,28]. This latter effect reduces the already low sieving effect even more. Furthermore, the effect of Donnan exclusion on the NaCl retention at these high NaCl concentration becomes more and more negligible at higher NaCl concentration for these polyamide membranes [11]. For the more open nanofiltration membranes (NTR-7450, NTR-7470, NP-030, UTC 60) [11,28], slightly lower (a few percent in absolute retention terms) NaCl retentions than expected based on the relation derived for Desal DK occur at NaCl concentrations between 1.5 and 3.5 mol·L^{-1}, whereas at higher NaCl concentrations NaCl retentions are similar for all membranes (see Supporting Information). The reason for this behavior is that at this lower NaCl concentration range the effect of membrane openness is observed and this effect cannot be counteracted by Donnan exclusion effects (not even for the sulfonated poly(ether)sulfone based NTR 7450 and NTR 7470) at these relatively high NaCl concentrations, whereas at higher NaCl concentration close to saturation even the NaCl retention for tight nanofiltration membranes are that low that NaCl retention differences between open and tight nanofiltration membranes disappear.

4.2. Determination of the NaCl chemical potential drops representing the resistance for NaCl transport through the membrane from single NaCl solution retentions

Based on the determined relation between the NaCl retention and the NaCl concentration in the concentrate (Eq. (32)), the chemical potential difference for NaCl transport has been determined for single NaCl solutions with different concentrations in concentrate (see Fig. 5 (left)) according to the procedure described earlier (see Fig. 1). Considering

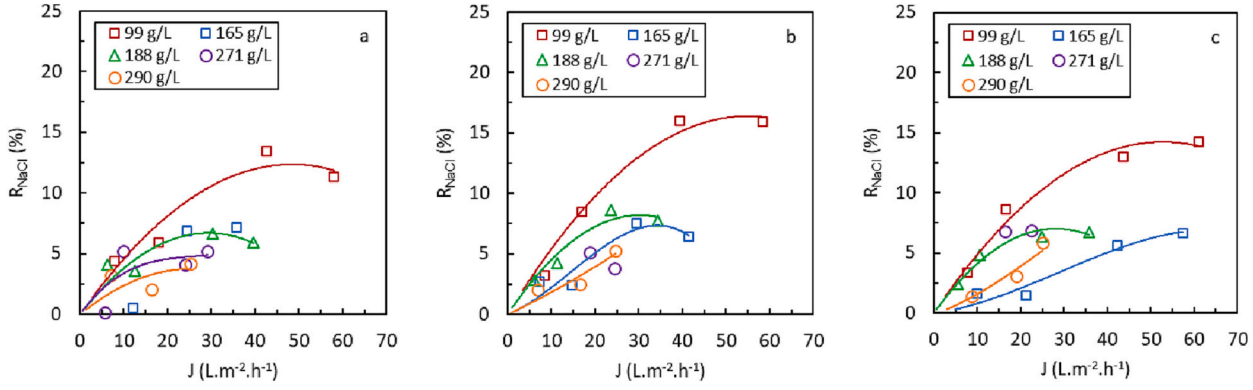

Fig. 3. NaCl retention as function of membrane flux for different NaCl concentrations in single salt solutions for Desal DK (a), Desal HL (b), NF-270 (c). Results for solutions with NaCl concentrations of 99 g·L^{-1}, 188 g·L^{-1} and 271 g·L^{-1} are based on experiments from [11].

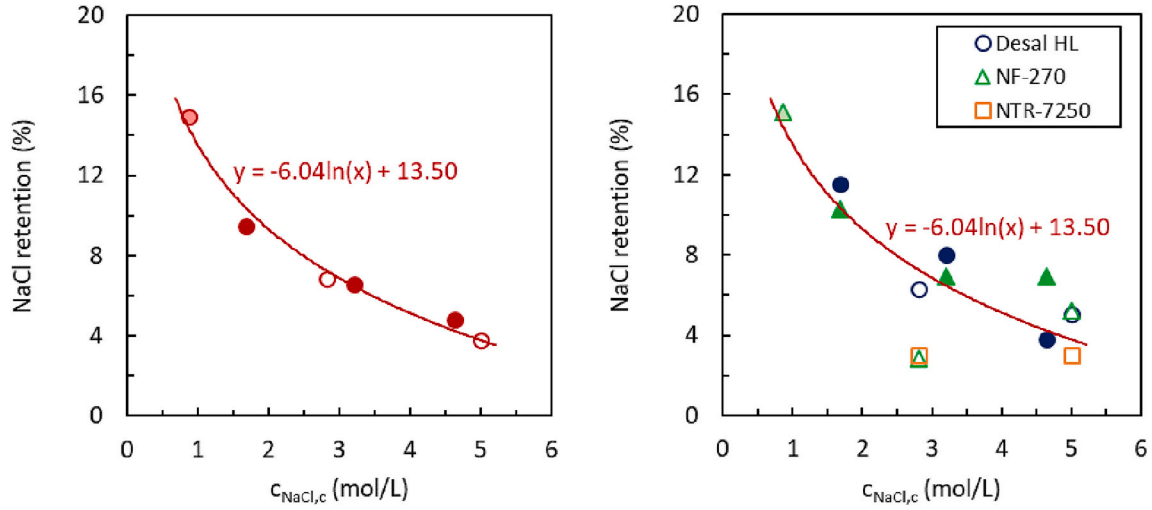

Fig. 4. NaCl retentions for single NaCl solutions with concentrations between 0.9 mol·L^{-1}–5.1 mol·L^{-1} (based on current experimental results (open symbols), results from [11] (filled symbols) and results from [50] (lightly filled symbol)) at a flux of 25 L•m^{-2}•h^{-1} with markers representing experimental data for Desal DK (left) and Desal HL, NF-270 and NTR-7250 (right) and the line representing the logarithmic trend line for the Desal DK experimental NaCl retention results at 25 L•m^{-2}•h^{-1} as function of the concentrate NaCl concentration.

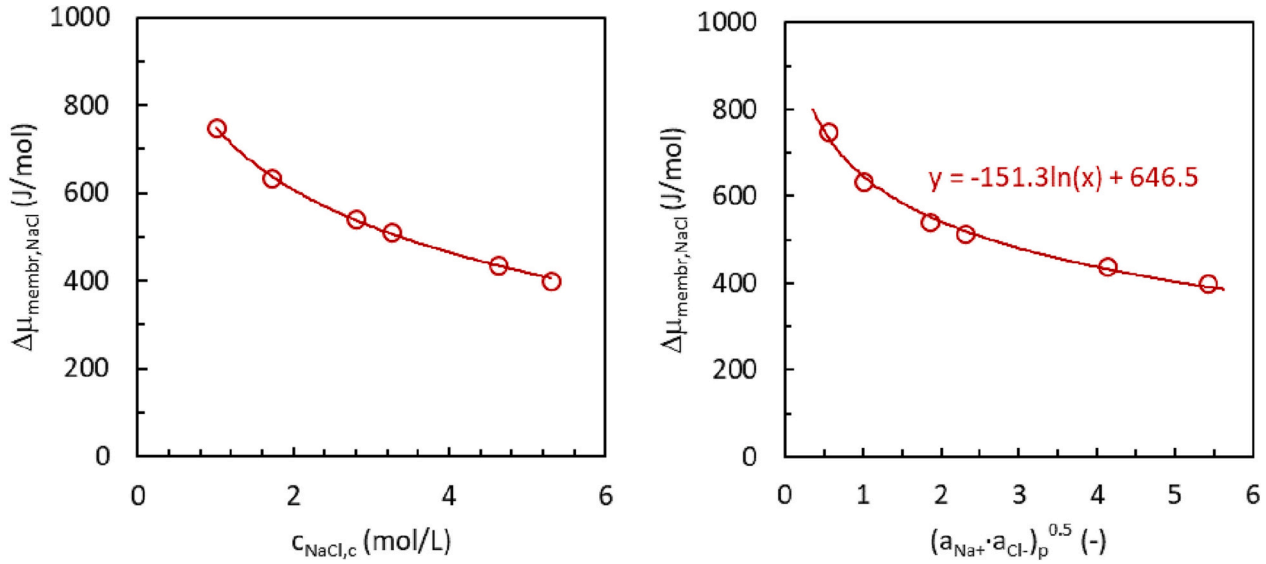

Fig. 5. The calculated chemical potential difference for transport of NaCl through a NF membrane based on the NaCl retention relation with the NaCl concentrate concentration as obtained for Desal DK (circle) and the trendline as function of the permeate NaCl activity at different pressures (right) and the concentrate NaCl concentration at P = 25 bar (left) for single salt NaCl solutions.

that the single NaCl solutions have a high salt concentration, the chemical potential difference is related to the NaCl activity of the obtained permeate solutions based on the Na^+ and Cl^- molalities and the mean activity coefficients ($(a_{Na^+} = \gamma_{NaCl}\cdot m_{Na^+})_p$ and $(a_{Cl^-} = \gamma_{NaCl}\cdot m_{Cl^-})_p$) for the permeate (see Fig. 5 (right)). For the determination of the chemical potential difference for NaCl transport a transmembrane pressure difference of 25 bar has been assumed, since the NaCl retentions applied to determine Eq. (32) were practically all determined at approximately $P = 25$ bar. This obtained chemical potential difference can be described as function of the NaCl activity of the permeate according to (see Fig. 5 (right)):

$$\Delta\mu_{membr,NaCl} = 646.5 - 151.3\cdot ln\left(\sqrt{(a_{Na^+}\cdot a_{Cl^-})_p}\right) \quad (33)$$

As can be seen from Fig. 5 (right), relatively low NaCl chemical potential differences are obtained (below 1 kJ·mol^{-1}) for the entire permeate NaCl activity range. This is, obviously, due to the relatively low NaCl retention for NaCl solutions featuring a high NaCl concentration and indicates that the nanofiltration membranes have a relatively low resistance for NaCl transport. Furthermore, it is evident that the $\Delta\mu_{membr,NaCl}$ levels off at higher permeate NaCl activity (see Fig. 5 (right)). The effect of the NaCl concentrate concentration on the chemical potential difference for NaCl shows a similar trend (see Fig. 5 (left)).

Based on the observed trend between the chemical potential difference for NaCl and the NaCl concentration in the concentrate (see Fig. 5 (left)), the chemical potential difference steeply decreases with increasing NaCl concentration in the concentrate at low NaCl concentration levels. Subsequently, the chemical potential difference for NaCl seems to level off when a concentration of 2 mol·L^{-1} has been achieved (see Fig. 5 (left)). Since Donnan exclusion and di-electric exclusion effects are expected to be less important at high salt concentrations, this

effect could be caused by relatively strong changes in the solute over membrane pore radius for NaCl concentrations lower than 2 mol·L^{-1} and reducing changes in this ratio when the NaCl concentration increases beyond that level. This hypothesis seems to be supported by observed changes in the ratio of the glucose radius over the pore radius ($\Delta\lambda$) with changes in the NaCl concentration of the solution processed for typical NF membranes fed with solutions containing glucose and NaCl [11]. For these mixed solutions it was reported that at relatively low NaCl concentrations (below 2.0 mol·L^{-1}) this ratio increases with increasing NaCl concentration, meaning that the membrane pore radius relative to the glucose radius increases, whereas this ratio remains relatively constant for NaCl concentrations higher than 3.0 mol·L^{-1} [11].

4.3. Prediction of the NaCl retention for concentrated NaCl – Na_2SO_4 mixtures based on the membrane resistance for NaCl transport obtained from single NaCl solution retentions

Based on the obtained function for $\Delta\mu_{membr,NaCl}$ (Eq. (33)), the NaCl retention has been predicted for different NaCl and Na_2SO_4 concentrations in concentrate at an assumed Na_2SO_4 retention of 98 % or 90 % and a trans-membrane pressure of 25 bar or 40 bar (see Fig. 2 for the applied procedure). In this procedure it was assumed that $\Delta\mu_{membr,NaCl}$ is solely dependent on the NaCl activity of the permeate, implying that this chemical potential difference – NaCl activity function determined for single NaCl salt solutions (as shown in Eq. (33)) can be used to predict NaCl retentions for mixed NaCl – Na_2SO_4 salt solutions as well. In Fig. 6 the predicted NaCl retentions are shown as function of the difference in Na_2SO_4 concentration between the concentrate and the permeate ($\Delta c_{Na_2SO_4}$), which is a common representation for solutions saturated in NaCl and containing Na_2SO_4 [19,28]. For a broad range of NaCl concentrations in the concentrate a reducing NaCl retention is observed when $\Delta c_{Na_2SO_4}$ is increased. For saturated NaCl solutions this has been explained by the salting-out effect of sodium sulfate on sodium chloride, resulting in increased transport of NaCl through the NF membrane [28,29]. The decrease in NaCl retention with increasing $\Delta c_{Na_2SO_4}$ is lower when the NaCl concentration is higher (see Fig. 6). This is caused by a combination of effects (changes in $\Delta\mu_{membr,NaCl}$, in the squared NaCl mean activity coefficients ratio ($\frac{\gamma^2_{NaCl,c}}{\gamma^2_{NaCl,p}}$), and the molar fraction of sulfate and chloride in the concentrate originating from changes in the Na_2SO_4 concentration at constant NaCl concentration in concentrate and leading to changes in the NaCl molality product in concentrate), as will be discussed below.

The membrane resistance for NaCl transport $\Delta\mu_{membr,NaCl}$, the first parameter affecting the NaCl retention, decreases with increasing NaCl concentration in the concentrate (see Fig. 7). This observed trend results from the established relation between $\Delta\mu_{membr,NaCl}$ and $c_{NaCl,c}$ for single NaCl salt solutions (see Fig. 5). This relation shows a relatively strong reduction when the NaCl concentration is increased from 0.9 mol·L^{-1} to 1.7 mol·L^{-1}, but gradually levels off via a natural logarithmic relation when the NaCl concentration of the concentrate is increased further, leading to an almost linear relation in the concentration range between 1.7 mol·L^{-1} and 5.2 mol·L^{-1} NaCl. This reducing membrane resistance for NaCl transport at higher NaCl concentration is commonly explained by increased charge shielding and lower Donnan exclusion or di-electric exclusion effects.

For all NaCl concentrations in the concentrate ($c_{NaCl,c}$) a gradual (small) reduction in $\Delta\mu_{membr,NaCl}$ with increasing $\Delta c_{Na_2SO_4}$ is observed (see Fig. 7). This gradual reduction is (again) ascribed to a gradual increase in charge shielding, and smaller Donnan - and di-electric exclusion effects due to the increase in sodium concentration at the membrane surface. This sodium concentration increase is due to the (slightly) higher Na_2SO_4 concentration ($c_{Na_2SO_4,c}$) at unchanged $c_{NaCl,c}$. A reduction of $\Delta\mu_{membr,NaCl}$ leads to an increased NaCl molality and consequently higher NaCl concentration in permeate (see Eq. (30)), thereby inducing a reduction in the NaCl retention (see Fig. 6) with increasing $\Delta c_{Na_2SO_4}$. For most NaCl concentrations evaluated the (squared) activity ratio ($\frac{\gamma^2_{NaCl,c}}{\gamma^2_{NaCl,p}}$), the second parameter affecting the Na^+ and Cl^- molalities in permeate and thus the NaCl retention (see Eq. (30)), is almost constant as function of $\Delta c_{Na_2SO_4}$. However, for low $c_{NaCl,c}$ this ratio reduces with increasing $\Delta c_{Na_2SO_4}$ (see Fig. 8). In that case the effect of a reducing $\Delta\mu_{membr,NaCl}$ on the NaCl molality in permeate is (partly or more than) offset by a decreasing activity ratio ($\frac{\gamma^2_{NaCl,c}}{\gamma^2_{NaCl,p}}$) (see Fig. 8 and Eq. (30)) for an increasing $\Delta c_{Na_2SO_4}$. For higher $c_{NaCl,c}$ the effect of $\Delta c_{Na_2SO_4}$ on the activity ratio ($\frac{\gamma^2_{NaCl,c}}{\gamma^2_{NaCl,p}}$) is less strong and therefore plays a less important role (see Fig. 8) on NaCl retention. The third parameter influencing the effect of $\Delta c_{Na_2SO_4}$ on the NaCl retention is the NaCl molality product of the concentrate $(m_{Na^+} \cdot m_{Cl^-})_c$. This molality product increases when the sulfate concentration in the concentrate is increased at constant NaCl concentration in the concentrate.

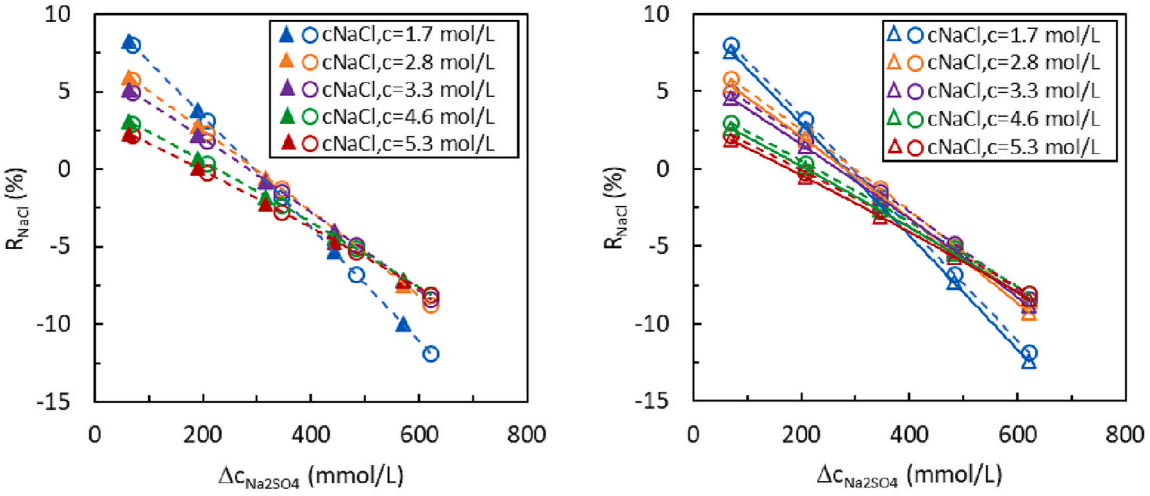

Fig. 6. NaCl retention predictions for different NaCl concentrations and Na_2SO_4 concentrations assuming a sulfate retention of either 98 % (open circles) or 90 % (filled triangles) taking a transmembrane pressure difference of 25 bar (left) and assuming an operating pressure of 25 bar (open circles) or 40 bar (open triangles) taking a sulfate retention of 98 % (right) based on the membrane resistance for NaCl transport (chemical potential drop) based on the NaCl activity of the permeate (Eq. (33)). Trendlines (dashed for 25 bar and solid for 40 bar both for 98 % sulfate retention) in the same color as the markers are to guide the eye.

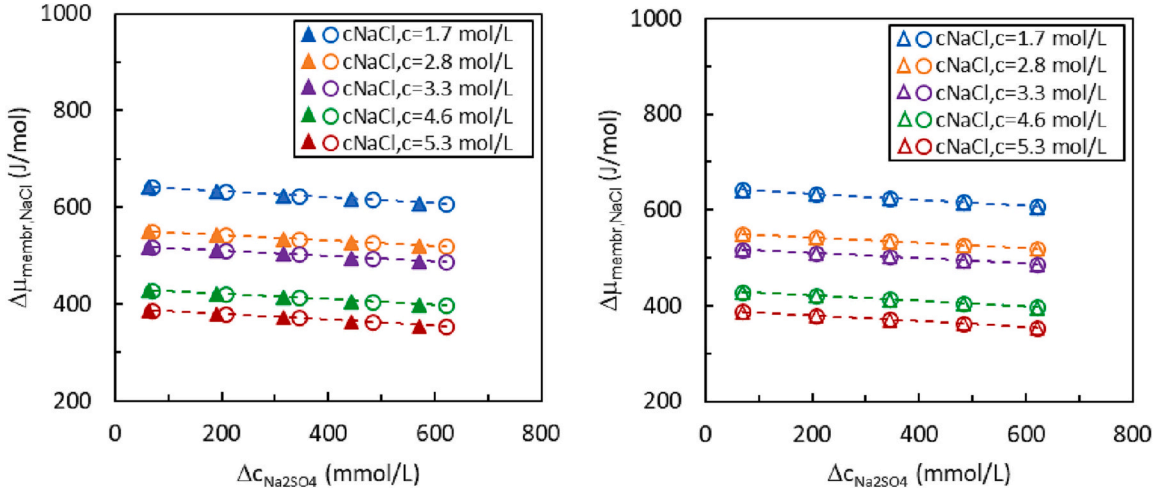

Fig. 7. The NaCl chemical potential difference as function of the difference in sodium sulfate concentration between the concentrate and permeate for solutions with different NaCl concentrate concentrations and a sodium sulfate retention of 98 % (open circle) or 90 % (filled triangle) at $P = 25$ bar (left), and for a pressure of 25 bar (open circle) or 40 bar (open triangle) at a sulfate retention of 98 % (right). Trendlines (dashed for 25 bar and 98 % sulfate retention) in the same color as the markers are to guide the eye.

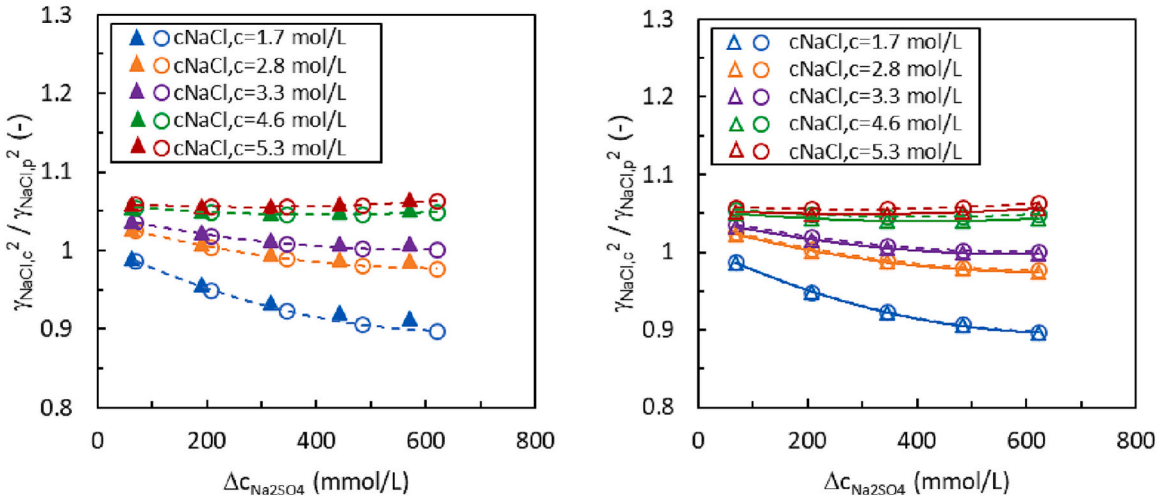

Fig. 8. The ratio of the squared mean NaCl activity coefficients for concentrate over permeate $\frac{\gamma^2_{NaCl,c}}{\gamma^2_{NaCl,p}}$ as function of the difference in sodium sulfate concentration between the concentrate and permeate $\Delta c_{Na_2SO_4}$ for solutions with different NaCl concentrate concentrations and a sodium sulfate retention of 98 % (open circle) or 90 % (filled triangle) at P = 25 bar (left) and for a pressure of 25 bar (open circle) or 40 bar (open triangle) at a sulfate retention of 98 %(right).

Furthermore, this parameter is linearly related to the NaCl molality product for the permeate $(m_{Na^+} \cdot m_{Cl^-})_p$ (see Eq. (30)). For a relatively low $c_{NaCl,c}$ this molality product increase is higher for the same increase in Na_2SO_4 concentration, since at a constant $c_{NaCl,c}$ and an increasing $c_{Na_2SO_4,c}$ the mole fraction ratio for sulfate over chloride $\frac{\left(x_{SO_4^{2-}}\right)_c}{(x_{Cl^-})_c}$ in the concentrate increases to a larger extent for solutions with relatively low $c_{NaCl,c}$, leading to a stronger increase in the $\frac{(x_{Na^+})_c}{(x_{Cl^-})_c}$ ratio. Consequently, at relatively low $c_{NaCl,c}$ an increase in $\Delta c_{Na_2SO_4}$ leads to a stronger increase in the NaCl molality product in permeate and therefore a stronger reduction in NaCl retention when only considering the effect of the NaCl molality product of the concentrate.

Especially this latter (NaCl molality product in concentrate change) effect leads to the stronger change in chloride retention with increasing $\Delta c_{Na_2SO_4}$ at lower $c_{NaCl,c}$. For increasing NaCl concentrations the effect of a changing $\Delta c_{Na_2SO_4}$ on NaCl retention becomes smaller. This is caused by the similarly reducing $\Delta\mu_{membr,NaCl}$ for increasing $\Delta c_{Na_2SO_4}$ for all $c_{NaCl,c}$ (see Fig. 7) in combination with a relatively lower increase in $\frac{\left(x_{SO_4^{2-}}\right)_c}{(x_{Cl^-})_c}$ with increasing sulfate concentration in concentrate for higher $c_{NaCl,c}$. The observed change in the activity ratio ($\frac{\gamma^2_{NaCl,c}}{\gamma^2_{NaCl,p}}$), from reducing with increasing $\Delta c_{Na_2SO_4}$ for low NaCl concentration to even slightly increasing with increasing $\Delta c_{Na_2SO_4}$ for high NaCl concentration in concentrate (see Fig. 8), is not sufficient to reverse this trend. For a specific case these effects are illustrated in more detail in the Supporting Information Fig. S8.

Based on the obtained modelling results it is evident that the sulfate retention, at least in the range of 90–98 %, does not affect the relation between the chloride retention and $\Delta c_{Na_2SO_4}$ at unchanged $c_{NaCl,c}$ (see Fig. 6 (left)). This results from the following:

- The assumption that $\Delta\mu_{membr,NaCl}$ only depends on the sodium chloride activity ($\sqrt{(a_{Na^+} \cdot a_{Cl^-})_p}$) of the permeate (see Fig. 5 (right) and

Eq. (33)) and its function of $\Delta c_{Na_2SO_4}$ is hardly affected when the sulfate retention is decreased from 98 % to 90 % (see Fig. 7 (left).

- The obtained $(\frac{\gamma^2_{NaCl,c}}{\gamma^2_{NaCl,p}})$ is close to 1 (within the range of 0.9–1.1) and its function of $\Delta c_{Na_2SO_4}$ is hardly affected by the sulfate retention (see Fig. 8 (left)).
- The dominating effect of the changing sulfate concentration in concentrate on the NaCl retention via the NaCl molality product in concentrate $(m_{Na^+} \cdot m_{Cl^-})_c$.

This result implies that for commercial applications even a gradual reduction in sulfate retention with time on stream from typically 98 % to 90 % should not lead to a strongly changing chloride retention other than that caused by the decreased $\Delta c_{Na_2SO_4}$. This modelling result seems to be in line with observations made for NF-270 and Desal 5DK membranes as reported in [19].

For a change in operating pressure from 25 bar to 40 bar only a marginally lower NaCl retention is predicted (see Fig. 6 (right)). This result is explained by the relatively small change in the product of the NaCl molar volume in permeate and the pressure difference between both sides of the membrane $(V_{m,p,NaCl} \cdot (P_c - P_p))$ caused by this change in pressure and the relatively small effect caused by $V_{m,p,NaCl} \cdot (P_c - P_p)$ in relation to the effect caused by $\Delta\mu_{membr,NaCl}$ in Eq. (30). Furthermore, negligible effects of the pressure on the activity coefficient ratio $(\frac{\gamma^2_{NaCl,c}}{\gamma^2_{NaCl,p}})$ are predicted (see Fig. 8 (right)).

As mentioned earlier, the ratio of the squared mean NaCl activity coefficients for concentrate over permeate is close to 1 (within the range of 0.9–1.1) for all results obtained at 25 bar transmembrane pressure for the NaCl concentration in concentrate range between 1.7 and 5.3 mol·L^{-1} and a $\Delta c_{Na_2SO_4}$ between 60 and 630 mmol·L^{-1} (see Fig. 8 (left)). This result means that the assumption that this activity coefficient ratio is close to 1 as used for specific cases in earlier studies related to nanofiltration of salt solutions saturated in NaCl [28,29] seems to be justified, or at least did not lead to substantial inaccuracies.

In the next section NaCl retention results obtained from experiments featuring nanofiltration of concentrated NaCl solutions containing Na_2SO_4 will be presented. These results will be used in a later section of this manuscript to validate the retention predictions presented for mixed salt solutions in this section.

4.4. Experimental NaCl retention results for NaCl – Na_2SO_4 salt solution mixtures required for validation of predicted chloride retentions

The effect of membrane flux on the NaCl retention for a NaCl – Na_2SO_4 salt solution mixture with 92 g·L^{-1} NaCl and different Na_2SO_4 concentrations for NF-270, NTR-7250 and Desal HL is shown in Fig. 9. The obtained NaCl retentions for these membranes are all in the range between −6 % and 20 % and are increasing with increasing membrane flux, a trend commonly found for nanofiltration membranes for mixtures with much lower solute concentrations as well [50].

An increase in sodium sulfate concentration in the mixture results in a lower NaCl retention for these membranes (see Fig. 9). For NaCl – Na_2SO_4 salt solution mixtures with a higher NaCl concentration of 170 g·L^{-1} NaCl or 290 g·L^{-1} NaCl and an even broader range of Na_2SO_4 concentrations (between 6.6 and 83.7 g·L^{-1}) similar trends are found (as illustrated for Desal HL in Fig. 10(a) and (c)), albeit that the NaCl retention range is smaller and lower than for lower NaCl concentrations (between −10 % and 10 %).

Sodium sulfate retentions for these mixtures steeply increase with increasing membrane flux for a membrane flux below 5–10 L·m^{-2}·h^{-1} and level off at $R_{Na2SO4} > 90$ % for higher membrane flux, as illustrated for Desal HL in Fig. 10(b) and (d) for a mixture containing 170 g·L^{-1} NaCl and 290 g·L^{-1} NaCl, respectively. This trend is in line with nanofiltration of NaCl – Na_2SO_4 mixtures with much lower concentrations [51–53]. The steep increase at low flux is explained by diffusion as the dominating transport effect, whereas at higher flux convection becomes the dominating transport phenomenon as can be understood from the commonly applied extended Nernst-Planck equation for the description of transport through nanofiltration membranes [5–7]. Explanations for the obtained experimental results will be provided later in this manuscript where the obtained results will be used to validate the results obtained from the proposed NaCl retention model.

4.5. Validation of predicted NaCl retentions for concentrated NaCl – Na_2SO_4 mixtures against experimental results

Validation of the obtained NaCl retention model predictions from the developed model with experimental results is required to check the accuracy of the proposed model description. Unfortunately, only limited nanofiltration experiments for concentrated NaCl – Na_2SO_4 solutions have been reported in open literature. Consequently, additional experiments have been performed as described in earlier experimental and results sections. Experimental NaCl retention results for which the membrane flux was between 10 and 35 L·m^{-2}·h^{-1} were mainly included in the validation of the model, since this flux range is typically applied in commercial nanofiltration applications to limit sulfate retention reductions caused by concentration polarization (at high flux) or diffusion as most important transport mechanism (at low flux) [28].

For relatively low NaCl concentrations in the concentrate (1.7 mol·L^{-1}), the predicted NaCl retention as function of $\Delta c_{Na_2SO_4}$ describes the experimental NaCl retentions relatively well, especially for NTR-7250 (see Fig. 11(a)). For this comparison experimental results for membranes with a flux in the range of 14–32 L·m^{-2}·h^{-1} were used. Measured NaCl retentions for Desal HL show a slightly stronger deviation from the predicted NaCl retention (see Fig. 11(a)). This higher NaCl

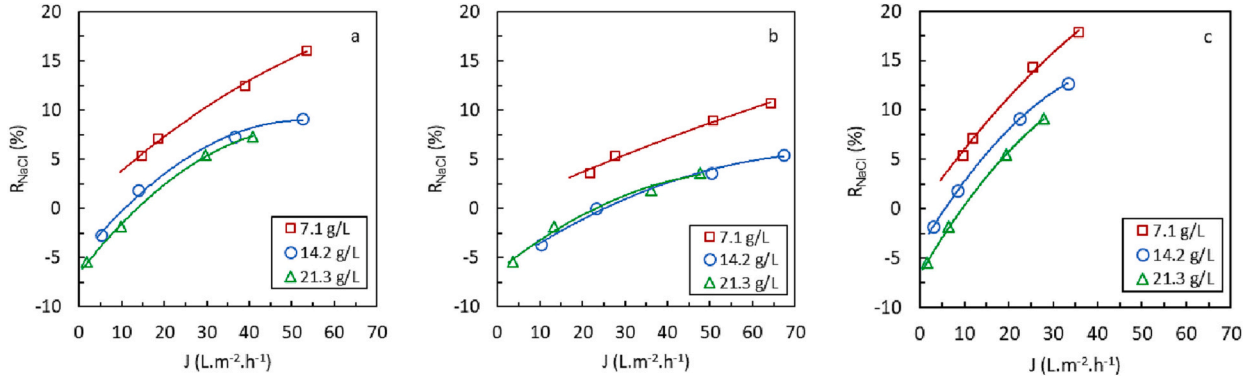

Fig. 9. NaCl retention as function of membrane flux for mixed salt solutions containing 92 g·L^{-1} NaCl and different Na_2SO_4 concentrations using NF270 (a), NTR-7250 (b) and Desal HL (c).

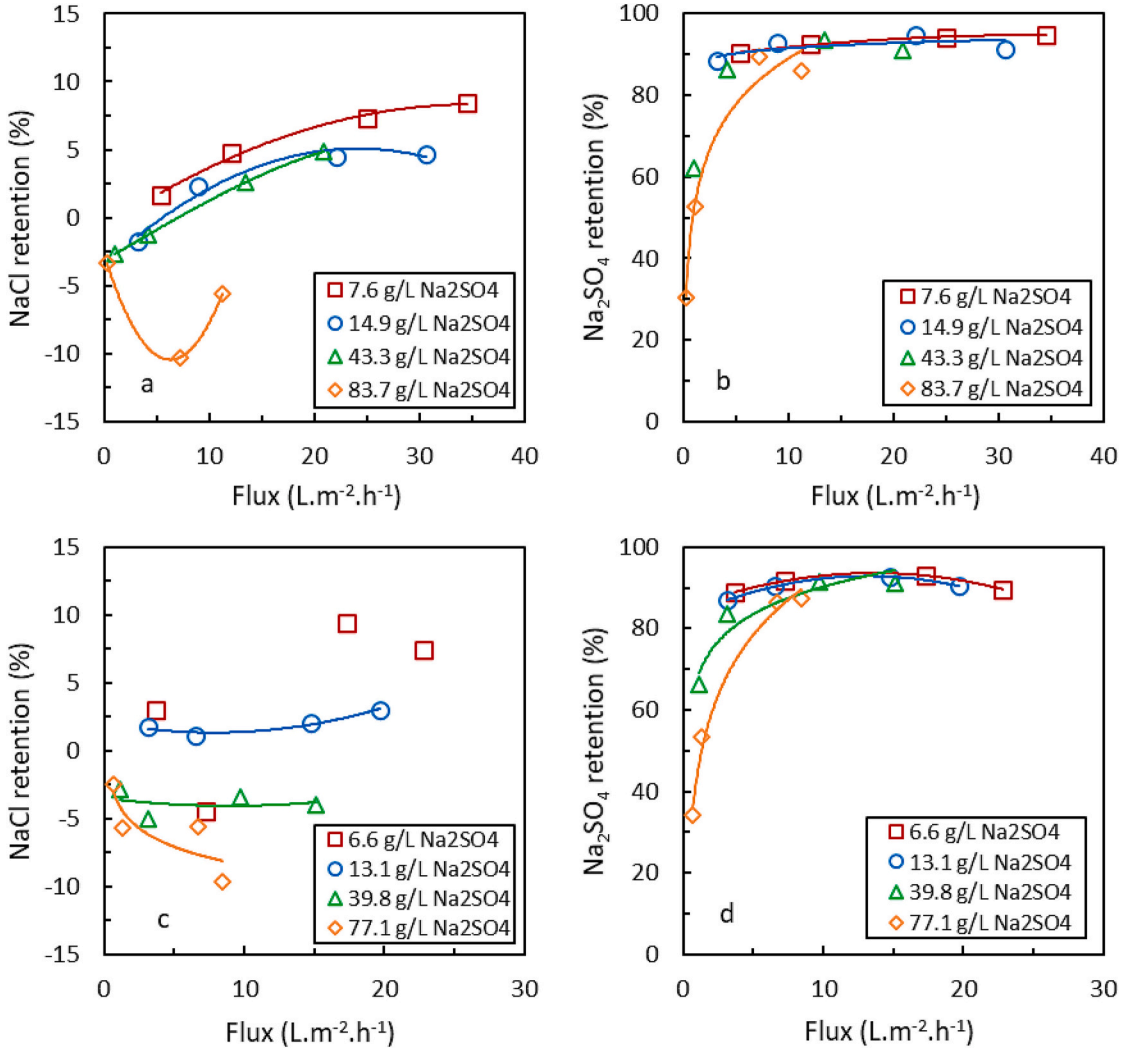

Fig. 10. NaCl retention as function of membrane flux for Desal HL using mixed salt solutions containing 170 g·L^{-1} NaCl (a) and 290 g·L^{-1} NaCl (c) and Na_2SO_4 retentions as function of membrane flux for Desal HL using mixed salt solutions containing 170 g·L^{-1} NaCl (b) and 290 g·L^{-1} NaCl (d) for Na_2SO_4 concentrations ranging from 6.6 to 84 g·L^{-1}. Lines are trendlines to guide the eye.

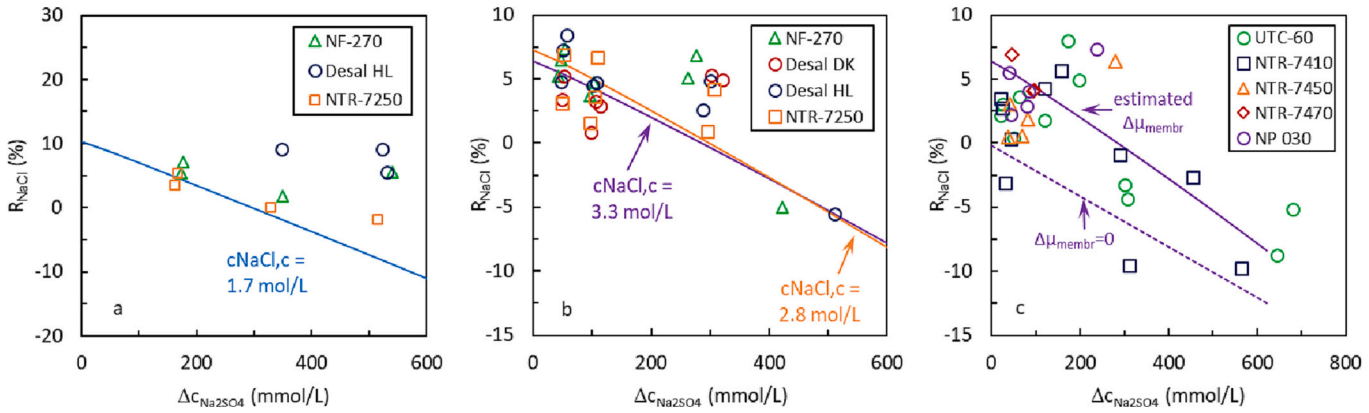

Fig. 11. Comparison of experimental NaCl retention results in the flux range between 10 and 35 L·m^{-2}·h^{-1} for several nanofiltration membranes (symbols) with model predictions for a NaCl concentration in concentrate of $c_{NaCl,c} = 1.7$ mol·L^{-1} (a), experimental and modelling results for several nanofiltration membranes with NaCl concentrations in the concentrate between $c_{NaCl,c} = 2.8$ mol·L^{-1} and $c_{NaCl,c} = 3.3$ mol·L^{-1} (b), and experimental and modelling results for other nanofiltration membranes for NaCl concentrations in the concentrate of $c_{NaCl,c} = 3.3$ mol·L^{-1}, all for the estimated $\Delta\mu_{membr,NaCl}$ based on Eq. (33) (continuous line) and a case where $\Delta\mu_{membr,NaCl}$ was estimated to be zero (dashed line), both at $P = 25$ bar (c).

retention for Desal HL is in line with the slightly higher NaCl retention obtained for this membrane at low NaCl concentration for single NaCl salt solutions (see Fig. 4 (right)), although in the latter case this deviation is smaller.

The NaCl retentions for Desal DK, Desal HL, NTR-7250 and NF-270 for solutions with NaCl concentrations between 2.8 and 3.3 mol·L^{-1} are predicted relatively well as function of $\Delta c_{Na_2SO_4}$ (see Fig. 11(b)). It should be noted that the experimental variation in NaCl retention, which is small, still seems to exceed the NaCl concentration effect predicted from the model in this NaCl concentration range between 2.8 and 3.3 mol·L^{-1}. For other nanofiltration membranes the proposed methodology also provides a proper first estimation of the NaCl retention (see Fig. 11 (c)), even though at low $\Delta c_{Na_2SO_4}$ some variation in NaCl retention is found. Furthermore, practically all experimental NaCl retention results are higher than the model prediction assuming that the resistance for NaCl transport is negligible ($\Delta\mu_{membr,NaCl} = 0$), indicating that even at this high NaCl concentration level some resistance for NaCl transport is still present (as expected based on single NaCl solution retention experiments).

For solutions with a $c_{NaCl,c}$ of 5.3 mol·L^{-1}, the NaCl retention results obtained for NF-270, Desal DK, Desal HL and NTR-7250 are lower than predicted based on the proposed model, especially at relatively high $\Delta c_{Na_2SO_4}$ (see Fig. 12 (left)). The experimentally obtained NaCl retentions are (more) in line with the earlier reported empirical correlation for NaCl solutions saturated in NaCl and containing Na_2SO_4, as determined from pilot trials using NF-270 and Desal DK membranes [19]. This empirical correlation, determined for Desal DK and NF-270 in situations where these membranes showed gradually reducing sulfate retentions with time on stream and corresponding gradual increases in NaCl retention [19] is only valid for (near) NaCl saturated solutions. Comparing the earlier determined empirical correlation [19] with our current modelling approach either using the relation for $\Delta\mu_{membr,NaCl}$ as defined by Eq. (33) or assuming $\Delta\mu_{membr,NaCl} = 0$ (see Fig. 13) indicates that for this high NaCl concentration in concentrate $\Delta\mu_{membr,NaCl}$ seems to decrease with increasing $\Delta c_{Na_2SO_4}$. This is concluded since the NaCl retention at low $\Delta c_{Na_2SO_4}$ is predicted accurately with the currently proposed model based on Eq. (33), whereas at higher $\Delta c_{Na_2SO_4}$ the empirical correlation [19], which is in line with experimental results (see Fig. 12), is more in line with results based on our model when assuming that $\Delta\mu_{membr,NaCl} = 0$. An explanation for the relatively low NaCl retentions at high $\Delta c_{Na_2SO_4}$ as obtained during the experiments could be the relatively low membrane flux for these conditions. As can be seen in Fig. 3a, relatively low flux leads to a relatively low NaCl retention for all NF membranes evaluated and consequently to a lower $\Delta\mu_{membr,NaCl}$. Furthermore, it should be noted that the differences in NaCl

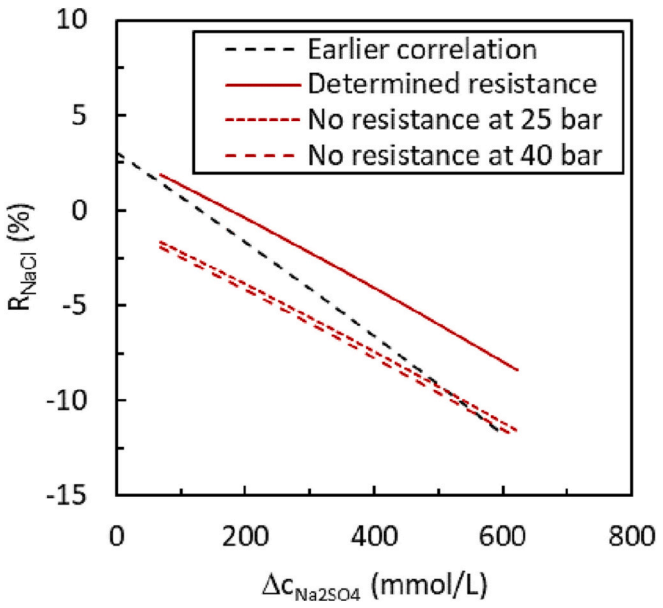

Fig. 13. Comparison of the current model with the determined resistance as function of the permeate NaCl activity for a transmembrane pressure of 25 bar with the earlier derived empirical correlation [19] and cases where $\Delta\mu_{membr,NaCl} = 0$ and the transmembrane pressure was either 25 bar or 40 bar. All results relate to a solution (practically) saturated in NaCl with a concentration of 5.3 mol·L^{-1}.

retentions between the two model approaches are still relatively small (only 5 % in absolute retention terms). Consequently, the newly developed model provides a proper first prediction of the NaCl retention for a broad range of NaCl concentrations in concentrate based on a given sodium sulfate concentration in concentrate and sodium sulfate retention.

Furthermore, the currently developed model provides a valuable extension of an empirical model [19] and earlier developed models based on thermodynamic considerations which were derived for (near) saturated NaCl solutions and assumed negligible membrane resistance for NaCl transport and either assumed a NaCl activity coefficients ratio of $\frac{\gamma^2_{NaCl,c}}{\gamma^2_{NaCl,p}} = 1$ [28] or determined this ratio from solid-liquid equilibria (NaCl crystallization experiments) [29]. The currently developed model fills the gap between these models and models based on the Maxwell-Stefan or the extended Nernst-Planck equation used for characterization purposes or (when including zeta potential data) for NaCl - Na_2SO_4

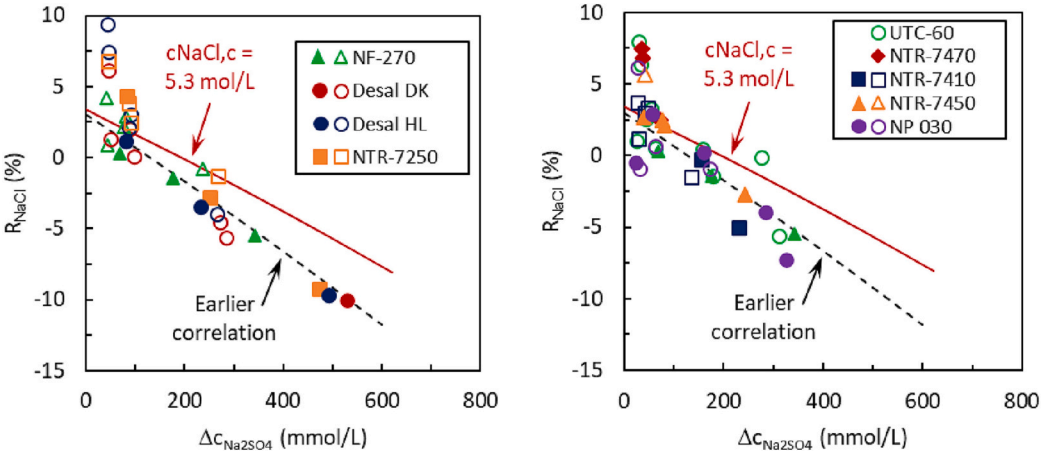

Fig. 12. NaCl retention for concentrates having a NaCl concentration of 4.8–5.3 mol·L^{-1} as function of $\Delta c_{Na_2SO_4}$. Comparison of current model predictions assuming a transmembrane pressure of 25 bar with an earlier derived empirical correlation for solutions with the same NaCl concentration range based on pilot trials using NF-270 and Desal DK membranes [19] and current experimental results for NF-270, Desal HL, Desal HL and NTR-7250 (left) and for UTC-60, NTR-7410, NTR-7450 and NTR-7470 (right). Open symbols represent results for a flux range between 10 and 35 L·m^{-2}·h^{-1} whereas filled symbols represent results for flux results in the range between 5 and 10 L·m^{-2}·h^{-1}.

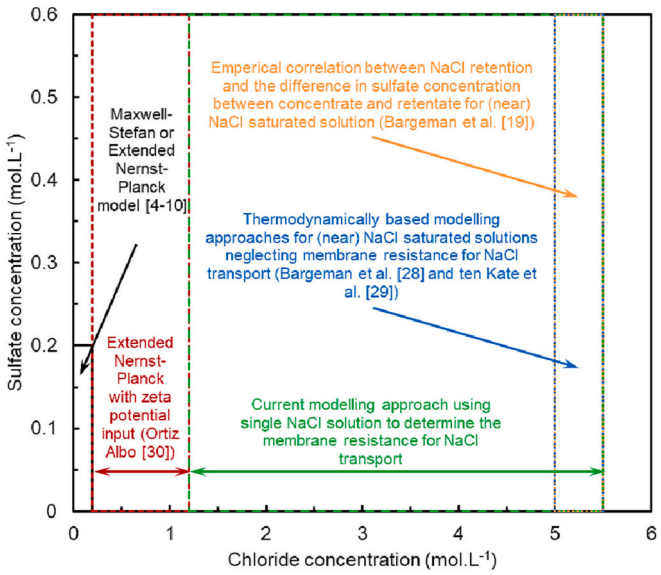

Fig. 14. Currently developed and earlier available membrane models for prediction of the NaCl retention for NF membranes for NaCl - Na_2SO_4 solutions at different concentration ranges.

solutions for NaCl concentrations up to 1.2 mol·L^{-1} (see Fig. 14). The model predicts the NaCl retention based on the relation for the membrane resistance for NaCl transport obtained from single NaCl retentions for Desal DK and needs the chloride and sulfate concentration in the concentrate and the sulfate retention as sole input parameters. The sulfate retention can be obtained experimentally or can be estimated from the relation between the sulfate retention and the membrane pore radius as discussed for a broad range of NF membranes in [28]. Furthermore, the NaCl retention model prediction was shown to be valid for a broad range of different NF membranes covering the MWCO space between 200 and 1000 Da.

5. Conclusions

A membrane modelling methodology has been developed for predicting the NaCl retention during nanofiltration of highly concentrated (≥1.2 mol·L^{-1}) NaCl solutions containing different levels of sodium sulfate. In the modelling approach the NaCl potential difference between the concentrate and permeate, representing the resistance for NaCl transport through the nanofiltration membrane, has been determined as a function of the sodium and chloride activities in the permeate for single salt NaCl solutions with different concentrations. The basis of the developed methodology for the prediction of NaCl retentions for solutions containing Na_2SO_4 next to NaCl is the assumption that for NaCl solutions with a concentration equal to or higher than 1.2 mol·L^{-1} this NaCl potential difference function for single salt NaCl solutions holds for NaCl solutions containing Na_2SO_4 as well. The developed methodology is an extension of a simpler modelling approach proposed earlier for (near) saturated NaCl solutions and it fills the gap between available model descriptions for NaCl retention predictions for more dilute NaCl solutions and for (near) saturated NaCl solutions.

Comparison between model predictions from the developed modelling methodology and experimental results determined in this study and available in open literature has proven the validity and value of the proposed methodology. The NaCl retention for NaCl - Na_2SO_4 mixtures could be predicted with sufficient accuracy for a wide range of NaCl (between 1.2 mol·L^{-1} and saturation) and Na_2SO_4 (between 0 and 0.7 mol·L^{-1}) concentrations. The NaCl - Na_2SO_4 mixture solution with the highest concentration of both salts is saturated in both salts, indicating the wide range of applicability of the developed model. Experimentally determined and modelled NaCl retentions were in close agreement, with deviations mostly within 5 % (in absolute retention terms), despite the wide variety of nanofiltration membranes evaluated, the broad experimental flux range used during the experimental program and neglecting the effect of flux on the membrane resistance for NaCl transport in the model. For the developed methodology the highest (although still acceptable) differences between predicted and experimentally determined NaCl retentions are obtained at very low membrane fluxes which are usually unacceptable for practical application. This is most likely also the reason why the predicted NaCl retentions based on the developed modelling approach deviate from an earlier proposed empirical correlation for (near) saturated NaCl solutions, where the effect of low flux was incorporated implicitly. The deviation between the developed modelling - and the experimental results for practically saturated solutions at relatively low membrane flux can be decreased when a lower membrane resistance for NaCl transport (closer to 0) than obtained from the correlation based on single NaCl solutions is assumed. This lower resistance for NaCl transport is in line with lower NaCl retentions for single NaCl salt solutions at lower pressure and consequently lower flux. A further refinement of the developed model could therefore be to incorporate the effect of flux on single NaCl solution NaCl retention and therefore NaCl transport resistance of the membrane. However, based on the relatively small deviation between the experimental and modelling results for the developed membrane, this further refinement will only lead to marginally improved predictions of the NaCl retention at the expense of an increased model complexity.

Nomenclature

Symbols

A^{φ}	Pitzer parameter [32,33]
a_{Cl^-}	Activity coefficient chloride (−)
a_{Na^+}	Activity coefficient sodium (−)
$a_{NaCl,p}$	Activity of NaCl in permeate (−)
b	Pitzer parameter [32,33]
C^{φ}	Pitzer parameter [32,33]
c_{Cl^-}	Chloride concentration (mol·L^{-1})
c_i	Concentration of compound i (mol·L^{-1})
$c_{i,c}$	Concentration of compound i in concentrate (mol·L^{-1})
$c_{i,p}$	Concentration of compound i in permeate (mol·L^{-1})
c_{Na^+}	Sodium concentration (mol·L^{-1})
$c_{NaCl,c}$	Concentration of NaCl in concentrate (mol·L^{-1})
$c_{NaCl,p,k}$	Concentration of NaCl in permeate after iteration step k (mol·L^{-1})
$c_{NaCl,p,k+1}$	Concentration of NaCl in permeate after iteration step k + 1 (mol·L^{-1})
$c_{NaCl,p}$	Concentration of NaCl in permeate (mol·L^{-1})
$f(a_{NaCl,p})$	Function of the NaCl activity in permeate
I	Ionic strength (mol·kg water^{-1})
m_{Cl^-}	Chloride molality (mol·kg water^{-1})
$m_{i,j}$	Molality compound i in solution j (mol·kg water^{-1})
m_{Na^+}	Sodium molality (mol·kg water^{-1})
m_{NaCl}	Sodium chloride molality (mol·kg water^{-1})
$m_{NaCl,p,k}$	Sodium chloride molality permeate from iteration k (mol·kg water^{-1})
$m_{NaCl,p,k+1}$	Sodium chloride molality permeate from iteration k + 1 (mol·kg water^{-1})
$m_{Na_2SO_4}$	Sodium sulfate molality (mol·kg water^{-1})
M_{H_2O}	Molar weight water (g·mol^{-1})
$M_{w,i}$	Molar weight compound i (g·mol^{-1})
P	Pressure (bar)
P_0	Reference pressure (bar)
P_c	Pressure of the concentrate (bar)
P_p	Pressure of the permeate (bar)

R	Gas constant (J·K^{-1}·mol^{-1})
R_i	Membrane retention for compound i (– or %)
R_{NaCl}	Membrane retention for NaCl (– or %)
T	Temperature (K)
$V_{m,c,i}$	Molar volume for compound i in concentrate (L·mol^{-1})
$V_{m,i}$	Molar volume for compound i (L·mol^{-1})
$V_{m,i,0}$	Molar volume parameter for compound i in Masson equation (L·mol^{-1})
$V_{m,i,1}$	Concentration related molar volume parameter for compound i in Masson equation (L·mol$^{-1.5}$)
$V_{m,p,i}$	Molar volume for compound i in permeate (L·mol^{-1})
$V_{m,p,NaCl}$	Molar volume for NaCl in permeate (L·mol^{-1})
$V_{m,sol}$	Molar volume solution (L·mol^{-1})
$w_{H_2O,c}$	Weight fraction water in concentrate (–)
$w_{i,c}$	Weight fraction of compound i in concentrate (–)
x	Molar fraction (–)
$x_{H_2O,j}$	Molar fraction of water in solution type j (–)
x_i	Molar fraction of compound i (–)
$x_{i,c}$	Molar fraction of compound i in concentrate (–)
$x_{i,j}$	Molar fraction of compound i in solution type j (–)
$y_{Na_2SO_4}$	Na_2SO_4 induced ionic strength over total ionic strength ratio (–)

Greek

$\beta^{(0)}$	Pitzer parameter [32,33]
$\beta^{(1)}$	Pitzer parameter [32,33]
γ_{Cl^-}	Molality related chloride activity coefficient
$\gamma_{NaCl,c}$	Molality related activity coefficient for NaCl in concentrate
$\gamma_{NaCl,p}$	Molality related activity coefficient for NaCl in permeate
γ_{Na^+}	Molality related sodium activity coefficient
ϑ_{ClSO_4}	Pitzer parameter [32,33]
$\Delta c_{Na_2SO_4}$	Difference in Na_2SO_4 concentration between the concentrate and the permeate (mmol·L^{-1})
$\Delta\Delta\mu_{membr,NaCl}$	Difference between $\Delta\mu_{membr,NaCl}$ obtained from Eq. (21) and $\Delta\mu_{membr,NaCl}$ obtained from Eq. (27)(J·mol^{-1})
$\Delta\lambda$	Difference in ratio of solute radius over pore radius (–)
$\Delta\mu_{membr,i}$	Chemical potential difference between the concentrate side and the permeate side of the membrane for compound i (J·mol^{-1})
$\Delta\mu_{membr,NaCl}$	Chemical potential difference between the concentrate side and the permeate side of the membrane for NaCl (J·mol^{-1})
$\mu_i(x,P,T)_c$	Chemical potential for compound i in concentrate as function of the specified composition, pressure, and temperature (J·mol^{-1})
$\mu_i(x,P,T)_p$	Chemical potential for compound i in permeate as function of the specified composition, pressure, and temperature (J·mol^{-1})
$\mu_i(x,P_0,T)_c$	Chemical potential for compound i in concentrate as function of the specified composition, reference pressure, and temperature (J·mol^{-1})
$\mu_i(x,P_0,T)_p$	Chemical potential for compound i in permeate as function of the specified composition, reference pressure, and temperature (J·mol^{-1})
μ^*_{NaCl}	Chemical potential for NaCl at reference conditions (J·mol^{-1})
ρ_{sol}	Solution density (kg·L^{-1})
$\rho_{sol,c}$	Solution density concentrate (kg·L^{-1})
$\rho_{sol,p}$	Solution density permeate (kg·L^{-1})
ψ_{NaClSO_4}	Pitzer parameter [32,33]

Subscripts

c	Concentrate
i	Compound i
j	Solution type (permeate or concentrate)
k	Iteration step number
p	Permeate

Abbreviations

Eq.	Equation
Fig.	Figure

CRediT authorship contribution statement

Gerrald Bargeman: Conceptualization, Validation, Methodology, Formal analysis, Data curation, Writing – original draft, Writing – review & editing, Visualization, Supervision, Project administration. **Olalla Guerra Miguez:** Investigation, Validation, Visualization. **Jan Barend Westerink:** Resources, Investigation. **Antoon ten Kate:** Methodology, Writing – review & editing.

Declaration of competing interest

The authors declare that they have no known competing financial interests or personal relationships that could have appeared to influence the work reported in this paper.

Data availability

Data will be made available on request.

Appendix A. Supplementary data

Supplementary data to this article can be found online at https://doi.org/10.1016/j.desal.2023.116562.

References

[1] A.I. Schäfer, A.G. Fane (Eds.), Nanofiltration: Principles, Applications, and New Materials, John Wiley & Sons, 2021.
[2] G. Bargeman, Recent developments in the preparation of improved nanofiltration membranes for extreme pH conditions, Sep. Purif. Technol. 279 (2021), 119725.
[3] N. Joseph, P. Ahmadiannamini, R. Hoogenboom, I.F. Vankelecom, Layer-by-layer preparation of polyelectrolyte multilayer membranes for separation, Polym. Chem. 5 (6) (2014) 1817–1831.
[4] J. Straatsma, G. Bargeman, H.C. van der Horst, J.A. Wesselingh, Can nanofiltration be fully predicted by a model? J. Membr. Sci. 198 (2) (2002) 273–284.
[5] W.R. Bowen, A.W. Mohammad, N. Hilal, Characterization of nanofiltration membranes for predictive purposes – use of salts, uncharged solutes and atomic force microscopy, J. Membr. Sci. 126 (1997) 91–105.
[6] S. Deon, P. Dutournie, P. Bourseau, Modeling nanofiltration with nernst-planck approach and polarization layer, AIChE J. 53 (2007) 1952–1969.
[7] J. Schaep, C. Vandecasteele, A.W. Mohammad, W.R. Bowen, Modelling the retention of ionic components for different nanofiltration membranes, Sep. Purif. Technol. 22–23 (2001) 169–179.
[8] A. Escoda, S. Deon, P. Fievet, Assessment of dielectric contribution in the modelling of multi-ionic transport through nanofiltration membranes, J. Membr. Sci. 378 (2011) 214–233.
[9] V. Hoshyargar, F. Fadaei, S. Nezameddin Ashrafizadeh, Mass transfer simulation of nanofiltration membranes for electrolyte solutions through generalized Maxwell-Stefan approach, Korean J. Chem. Eng. 32 (2015) 1388–1404.
[10] W.R. Bowen, A.W. Mohammad, Characterization and prediction of nanofiltration membrane performance – a general assessment, Trans. IChemE. 76 (Part A) (1998) 885–893.
[11] G. Bargeman, J.B. Westerink, O. Guerra Miguez, M. Wessling, The effect of NaCl and glucose concentration on retentions for nanofiltration membranes processing concentrated solutions, Sep. Purif. Technol. 134 (2014) 46–57.
[12] G. Bargeman, J.M. Vollenbroek, J. Straatsma, C.G.P.H. Schoën, R.M. Boom, Nanofiltration of multi-component feeds. Interactions between neutral and charged components and their effect on retention, J. Membr. Sci. 247 (2005) 11–20.
[13] A. Bouchoux, H. Roux-de Balmann, F. Lutin, Nanofiltration of glucose and sodium lactate solutions: variations of retention between single-and mixed-solute solutions, J. Membr. Sci. 258 (1–2) (2005) 123–132.
[14] J. Luo, Y. Wan, Effect of pH and salt on nanofiltration – a critical review, J. Membr. Sci. 438 (2013) 18–28.
[15] M. Nilsson, G. Trägårdh, K. Östergren, The influence of pH, salt and temperature on nanofiltration performance, J. Membr. Sci. 312 (1–2) (2008) 97–106.

[16] P.A.B. Diaz, F. de Araujo Kronemberger, A.C. Habert, Predictive study of succinic acid transport via nanofiltration membranes using a Maxwell-Stefan approach, J. Chem. Technol. Biotechnol. 96 (3) (2021) 785–800.
[17] A. Escoda, P. Fievet, S. Lakard, A. Szymczyk, S. Déon, Influence of salts on the rejection of polyethyleneglycol by an NF organic membrane: pore swelling and salting-out effects, J. Membr. Sci. 347 (1–2) (2010) 174–182.
[18] M. Kyburz, G.W. Meindersma, G. Bargeman, Nanofiltration in the chemical processing industry, in: Nanofiltration: Principles, Applications, and New Materials 2, 2021, pp. 543–597.
[19] G. Bargeman, M. Steensma, A. ten Kate, J.B. Westerink, R.L.M. Demmer, H. Bakkenes, C.F.H. Manuhutu, Nanofiltration as energy-efficient solution for sulfate waste in vacuum salt production, Desalination 245 (1–3) (2009) 460–468.
[20] A. Pérez-González, R. Ibáñez, P. Gómez, A.M. Urtiaga, I. Ortiz, J.A. Irabien, Nanofiltration separation of polyvalent and monovalent anions in desalination brines, J. Membr. Sci. 473 (2015) 16–27.
[21] D. Bessarabov, Z. Twardowski, Industrial application of nanofiltration – new perspectives, Membr. Technol. 9 (2002) 6–9.
[22] W.M. Samhaber, H. Schwaiger, The application of nanofiltration in the salt industry, in: Proceedings of 14th International Congress of Chemical and Process Engineering (CHISA2000), Prague, August 2000, 2000.
[23] A. Pérez-González, R. Ibáñez, P. Gómez, A. Urtiaga, I. Ortiz, Integration of nanofiltration for the sustainable management of reverse osmosis brines, Chem. Eng. Trans. 39 (2014) 85–90.
[24] X. Li, S. Tan, J. Luo, M. Pinelo, Nanofiltration for separation and purification of saccharides from biomass, Front. Chem. Sci. Eng. 15 (4) (2021) 837–853.
[25] A.K. Goulas, P.G. Kapasakalidis, H.R. Sinclair, R.A. Rastall, A.S. Grandison, Purification of oligosaccharides by nanofiltration, J. Membr. Sci. 209 (1) (2002) 321–335.
[26] E. Sjöman, M. Mänttäri, M. Nyström, H. Koivikko, H. Heikkilä, Separation of xylose from glucose by nanofiltration from concentrated monosaccharide solutions, J. Membr. Sci. 292 (1–2) (2007) 106–115.
[27] J. Wang, Y. Ren, H. Zhang, J. Luo, J.M. Woodley, Y. Wan, Targeted modification of polyamide nanofiltration membrane for efficient separation of monosaccharides and monovalent salt, J. Membr. Sci. 628 (2021), 119250.
[28] G. Bargeman, J.B. Westerink, C.F.H. Manuhutu, A. ten Kate, The effect of membrane characteristics on nanofiltration membrane performance during processing of practically saturated salt solutions, J. Membr. Sci. 485 (2015) 112–122.
[29] A.J.B. ten Kate, M.A.I. Schutyser, B. Kuzmanovic, J.B. Westerink, F. Manuhutu, G. Bargeman, Thermodynamic perspective on negative retention effects in nanofiltration of concentrated sodium chloride solutions, Sep. Purif. Technol. 250 (2020), 117242.
[30] P. Ortiz-Albo, R. Ibañez, A. Urtiaga, I. Ortiz, Phenomenological prediction of desalination brines nanofiltration through the indirect determination of zeta potential, Sep. Purif. Technol. 210 (2019) 746–753.
[31] G. Bargeman, Creating saturated sodium chloride solutions through osmotically assisted reverse osmosis, Sep. Purif. Technol. 121113 (2022).
[32] K.S. Pitzer, G. Mayorga, Thermodynamics of electrolytes. II. Activity and osmotic coefficients for strong electrolytes with one or both ions univalent, J. Phys. Chem. 77 (19) (1973) 2300–2308.
[33] K.S. Pitzer, J.J. Kim, Thermodynamics of electrolytes.: IV. Activity and osmotic coefficients for mixed electrolytes, J. Am. Chem. Soc. 96 (1974) 5701–5707.
[34] J.H.G. van der Stegen, H. Weerdenburg, A.J. van der Veen, J.A. Hogendoorn, G. F. Versteeg, Application of the pitzer model for the estimation of activity coefficients of electrolytes in ion selective membranes, Fluid Phase Equilib. 157 (2) (1999) 181–196.
[35] B. Van der Bruggen, B. Daems, D. Wilms, C. Vandecasteele, Mechanisms of retention and flux decline for the nanofiltration of dye baths from the textile industry, Sep. Purif. Technol. 22 (2001) 519–528.
[36] B. Van der Bruggen, C. Vandecasteele, T. Van Gestel, W. Doyen, R. Leysen, A review of pressure-driven membrane processes in wastewater treatment and drinking water production, Environ. Prog. 22 (1) (2003) 46–56.
[37] A.W. Mohammad, N. Hilal, H. Al-Zoubi, N.A. Darwish, Prediction of permeate fluxes and rejections of highly concentrated salts in nanofiltration membranes, J. Membr. Sci. 289 (1–2) (2007) 40–50.
[38] M. Khraisheh, N. Dawas, M.S. Nasser, M.J. Al-Marri, M.A. Hussien, S. Adham, G. McKay, Osmotic pressure estimation using the Pitzer equation for forward osmosis modelling, Environ. Technol. 41 (19) (2020) 2533–2545.
[39] F. Sirbu, O. Iulian, A.C. Ion, I. Ion, Activity coefficients of electrolytes in the NaCl + Na2SO4 + H2O ternary system from potential difference measurements at (298.15, 303.15, and 308.15) K, J. Chem. Eng. Data 56 (12) (2011) 4935–4943.
[40] Y. Lin, A. ten Kate, M. Mooijer, J. Delgado, P.L. Fosbøl, K. Thomsen, Comparison of activity coefficient models for electrolyte systems, AIChE J. 56 (5) (2010) 1334–1351.
[41] G.M. Kontogeorgis, B. Maribo-Mogensen, K. Thomsen, The debye-Hückel theory and its importance in modeling electrolyte solutions, Fluid Phase Equilib. 462 (2018) 130–152.
[42] H.C. van der Horst, J.M.K. Timmer, T. Robbertsen, J. Leenders, Use of nanofiltration for concentration and demineralization in the dairy industry: model for mass transport, J. Membr. Sci. 104 (1995) 205.
[43] Information provided by membrane supplier NADIR.
[44] Information provided by membrane supplier KOCH.
[45] Information provided by membrane supplier ROMEMBRA.
[46] T.D. Waite, Chemical speciation effects in nanofiltration separation, in: A. I. Schäfer, A.G. Fane, T.D. Waite (Eds.), Nanofiltration – Principles and Applications, Elsevier Ltd, Oxford, UK, 2005, pp. 147–168. Chapter 7.
[47] J.M.M. Peeters, Characterization of Nanofiltration Membranes, 1997. PhD thesis Enschede.
[48] S. Kim, H. Ozaki, J. Kim, Effect of pH on the rejection of inorganic salts and organic compound using nanofiltration membrane, Korean J. Chem. Eng. 23 (1) (2006) 28–33.
[49] R. Schlesinger, G. Götzinger, H. Sixta, A. Friedl, M. Harasek, Evaluation of alkali resistant nanofiltration membranes for the separation of hemicellulose from concentrated alkaline process liquors, Desalination 192 (2006) 303–314.
[50] J. Tanninen, M. Mänttäri, M. Nyström, Effect of salt mixture concentration on fractionation with NF membranes, J. Membr. Sci. 283 (1–2) (2006) 57–64.
[51] A. Yaroshchuk, X. Martínez-Lladó, L. Llenas, M. Rovira, J. de Pablo, J. Flores, P. Rubio, Mechanisms of transfer of ionic solutes through composite polymer nanofiltration membranes in view of their high sulfate/chloride selectivities, Desalin. Water Treat. 6 (1–3) (2009) 48–53.
[52] A. Yaroshchuk, X. Martínez-Lladó, L. Llenas, M. Rovira, J. de Pablo, Solution-diffusion-film model for the description of pressure-driven trans-membrane transfer of electrolyte mixtures: one dominant salt and trace ions, J. Membr. Sci. 368 (1–2) (2011) 192–201.
[53] Z.Q. Yan, L.M. Zeng, Q. Li, T.Y. Liu, H. Matsuyama, X.L. Wang, Selective separation of chloride and sulfate by nanofiltration for high saline wastewater recycling, Sep. Purif. Technol. 166 (2016) 135–141.